Corticospinal-specific HCN expression in mouse motor cortex: I_h-dependent synaptic integration as a candidate microcircuit mechanism involved in motor control

Patrick L. Sheets, Benjamin A. Suter, Taro Kiritani, C. Savio Chan, D. James Surmeier and Gordon M. G. Shepherd

J Neurophysiol 106:2216-2231, 2011. First published 27 July 2011; doi:10.1152/jn.00232.2011

Journal of Neurophysiology publishes original articles on the function of the nervous system. It is published 12 times a year (monthly) by the American Physiological Society, 9650 Rockville Pike, Bethesda MD 20814-3991. ISSN: 0022-3077, ESSN: 1522-1598. Visit our website at http://www.the-aps.org/.

J Neurophysiol 106: 2216–2231, 2011.
First published July 27, 2011; doi:10.1152/jn.00232.2011.

Corticospinal-specific HCN expression in mouse motor cortex: I_h-dependent synaptic integration as a candidate microcircuit mechanism involved in motor control

Patrick L. Sheets, Benjamin A. Suter, Taro Kiritani, C. Savio Chan, D. James Surmeier, and Gordon M. G. Shepherd

Department of Physiology, Feinberg School of Medicine, Northwestern University, Chicago, Illinois

Submitted 16 March 2011; accepted in final form 24 July 2011

Sheets PL, Suter BA, Kiritani T, Chan CS, Surmeier DJ, Shepherd GM. Corticospinal-specific HCN expression in mouse motor cortex: I_h-dependent synaptic integration as a candidate microcircuit mechanism involved in motor control. *J Neurophysiol* 106: 2216–2231, 2011. First published July 27, 2011; doi:10.1152/jn.00232.2011.—Motor cortex is a key brain center involved in motor control in rodents and other mammals, but specific intracortical mechanisms at the microcircuit level are largely unknown. Neuronal expression of hyperpolarization-activated current (I_h) is cell class specific throughout the nervous system, but in neocortex, where pyramidal neurons are classified in various ways, a systematic pattern of expression has not been identified. We tested whether I_h is differentially expressed among projection classes of pyramidal neurons in mouse motor cortex. I_h expression was high in corticospinal neurons and low in corticostriatal and corticocortical neurons, a pattern mirrored by mRNA levels for HCN1 and Trip8b subunits. Optical mapping experiments showed that I_h attenuated glutamatergic responses evoked across the apical and basal dendritic arbors of corticospinal but not corticostriatal neurons. Due to I_h, corticospinal neurons resonated, with a broad peak at ~4 Hz, and were selectively modulated by α-adrenergic stimulation. I_h reduced the summation of short trains of artificial excitatory postsynaptic potentials (EPSPs) injected at the soma, and similar effects were observed for short trains of actual EPSPs evoked from layer 2/3 neurons. I_h narrowed the coincidence detection window for EPSPs arriving from separate layer 2/3 inputs, indicating that the dampening effect of I_h extended to spatially disperse inputs. To test the role of corticospinal I_h in transforming EPSPs into action potentials, we transfected layer 2/3 pyramidal neurons with channelrhodopsin-2 and used rapid photostimulation across multiple sites to synaptically drive spiking activity in postsynaptic neurons. Blocking I_h increased layer 2/3-driven spiking in corticospinal but not corticostriatal neurons. Our results imply that I_h-dependent synaptic integration in corticospinal neurons constitutes an intracortical control mechanism, regulating the efficacy with which local activity in motor cortex is transferred to downstream circuits in the spinal cord. We speculate that modulation of I_h in corticospinal neurons could provide a microcircuit-level mechanism involved in translating action planning into action execution.

pyramidal neuron; corticospinal; hyperpolarization-activated, cyclic nucleotide-gated cation channels; corticostriatal

THIS STUDY COMPRISES TWO RELATED sets of experiments, focusing first on characterizing hyperpolarization-activated current (I_h) expression in corticospinal neurons in mouse motor cortex and then on the role of I_h in modulating synaptic integration in corticospinal neurons.

I_h powerfully shapes the integrative properties of many neurons throughout the nervous system (Llinás 1988; Lüthi and McCormick 1998; Robinson and Siegelbaum 2003; Wahl-Schott and Biel 2009). In cortical pyramidal neurons, I_h stabilizes the resting membrane potential and influences the kinetics and propagation of synaptic responses (Berger et al. 2001; Magee 1998, 1999; Nicoll et al. 1993; Spain et al. 1987; Williams and Stuart 2000). In the neocortex, where neurons are often identified by the cortical layer of the soma, I_h has been investigated mostly in layer 5 pyramidal neurons. However, another determinant of neuronal identity for neocortical pyramidal neurons is their long-range axonal target (Brown and Hestrin 2009a; Kasper et al. 1994; Mason and Larkman 1990; Molnár and Cheung 2006; Watakabe 2009). Studies of retrogradely labeled neocortical pyramidal neurons have revealed a variety of highly distinct intrinsic and synaptic circuit properties (Anderson et al. 2010; Brown and Hestrin 2009b; Christophe et al. 2005; Hattox and Nelson 2007; Kasper et al. 1994; Le Bé et al. 2007; Morishima and Kawaguchi 2006; Tseng and Prince 1993), suggesting that projection class can be an important parameter for understanding patterns of I_h expression among neocortical pyramidal neurons. Indeed, a recent study has shown this to be the case for two types of projection neurons (corticocortical and corticopontine neurons) in the medial agranular cortex of the rat (Dembrow et al. 2010).

Corticospinal neurons are a key class of layer 5B projection neurons, conveying cortical information monosynaptically to the spinal circuits involved in motor control (Lemon 2008; Phillips and Porter 1977). In the cat motor cortex, Betz cells—large layer 5B neurons in motor cortex assumed to project to the spinal cord (Betz 1874)—express I_h (Spain 1994; Spain et al. 1987; Stafstrom et al. 1984). In recordings from awake-behaving primates, one class of motor cortical neurons displays characteristic post-spike rebound potentials consistent with I_h (Chen and Fetz 2005). In the rat motor cortex, corticospinal neurons exhibit subthreshold membrane properties consistent with I_h (Tseng and Prince 1993). However, expression of I_h in corticospinal neurons has not been quantified, either in the mouse, where many corticospinal-related disease models are available, or compared with other classes of projection neurons in motor cortex. This is important to resolve, because I_h could endow corticospinal neurons with distinct functional properties relevant for motor control. Here, we used a combination of methods to study I_h expression in corticospinal neurons and for

Address for reprint requests and other correspondence: P. L. Sheets, Dept. of Physiology, Morton 5-660, Northwestern Univ., 303 East Chicago Ave., Chicago, IL 60611(e-mail: p-sheets@northwestern.edu).

comparison, corticostriatal and corticocortical neurons. We found that I_h is highly enriched in corticospinal neurons, that its expression is specific to projection class, and that it endows these motor neurons with distinct electrophysiological properties and with a neuromodulatory target of adrenergic signaling.

In a second set of experiments, we explored the I_h-dependent synaptic integrative properties of corticospinal neurons, motivated by the possibility that these could constitute a microcircuit-level mechanism in motor control. Microcircuits in mammalian motor cortex are thought to be centrally involved in motor control (Georgopoulos and Stefanis 2010). However, details of the input-output operations performed by motor cortex microcircuits remain largely unknown. The activity of corticospinal neurons can be strongly modulated during movement (Phillips and Porter 1977). However, the neuronal mechanisms by which this modulation occurs have not been identified.

Adding to the complexity of the problem is the fact that corticospinal neurons are one among many neuronal classes in the motor cortex (Keller 1993). The activity of noncorticospinal neurons can also be modulated by movement (Beloozerova et al. 2003a, b; Isomura et al. 2009; Kaufman et al. 2010; Turner and DeLong 2000). Furthermore, motor cortex activity increases in the preparatory (action planning) stages of movement, well before action execution (Churchland et al. 2010; Cohen et al. 2010). Indeed, motor cortex activity is ongoing, as manifest both in the basal firing rates of individual neurons and in ongoing cortical rhythms (Hari 2002).

The activity of corticospinal neurons can evidently be low during states where motor cortex activity is high. Functional imaging studies demonstrate that areas of primary motor cortex (M1), which are activated during movement tasks, are also activated during imagery of a movement involving the same muscles (Press et al. 2011; Roth et al. 1996). This is intriguing, because it indicates a flexible association between local activity in the motor cortex and spiking output of corticospinal neurons (Stamos et al. 2010). Therefore, we hypothesize that some mechanism(s) must exist at the microcircuit level for modulating the input-output operations in synaptic microcircuits converging on corticospinal neurons, thereby regulating the output of the motor cortex to the spinal cord.

Recently, electroanatomical studies of mouse motor cortex have revealed strong excitatory projections from layer 2/3 to layer 5A/B (Hooks et al. 2011; Sheets and Shepherd 2011; Shepherd 2009; Yu et al. 2008). In layer 5B, this microcircuit preferentially targets corticospinal neurons over corticostriatal neurons (Anderson et al. 2010). These circuit-mapping studies suggest a simple model for excitatory flow within motor cortex, consisting of a relatively strong loop involving the upper layers, which projects mostly unidirectionally downward to the middle and lower layers, including layer 5B and its corticospinal neurons (Weiler et al. 2008). This model suggests the possibility that modulation of the "top-down" laminar flow of excitation, from upper to lower layers, could regulate the output of the motor cortex to the spinal cord (Weiler et al. 2008).

Electrophysiological studies of corticospinal neurons have long suggested distinct intrinsic properties (Chen et al. 1996; Miller et al. 2008; Spain 1994; Spain et al. 1987; Stafstrom et al. 1984; Tseng and Prince 1993). The combination of the corticospinal-specific electrophysiology (I_h-dependent intrinsic properties, as demonstrated in the first part of this study) and local circuit organization (as shown previously; discussed above in preceding paragraph) presents the possibility of a specific microcircuit-level mechanism for motor control: that the spiking activity of corticospinal neurons is selectively modulated by I_h-dependent integration of local excitatory inputs from layer 2/3 pyramidal neurons. Therefore, in the latter part of this study, we directly tested this hypothesis in a series of brain-slice experiments and found multiple lines of evidence supporting this idea.

MATERIALS AND METHODS

Retrograde Labeling

Animal studies were conducted in accordance with the animal care and use guidelines of Northwestern University, National Institutes of Health, and Society for Neuroscience. At *postnatal day 21*, mice (C57Bl/6J; The Jackson Laboratory, Bar Harbor, ME) of either gender underwent injection of fluorescent beads (red or green RetroBeads, Lumafluor, Naples, FL) into brain or spinal cord locations as described below. Mice were anesthetized with 1.5% isoflurane in 100% O_2 with a flow rate of 0.6 L/min (SurgiVet Isotech 4, Smiths Medical, Norwell, MA). Body temperature was maintained at 37°C using a feedback-controlled heating pad (FHC, Bowdoin, ME). The head was stabilized in a stereotaxic frame (900 series, David Kopf Instruments, Tujunga, CA). Pipettes for injections were fabricated from calibrated micropipets (Wiretrol II, 5-000-2010, Drummond Scientific, Broomall, PA) using a vertical puller (model PP-830, Narishige, Japan). The pipette was advanced to the intracranial or intraspinal target, and submicroliter volumes (~500 nL; undiluted) of fluorescent beads were injected using a Picospritzer III (Parker Instruments, Cleveland, OH; 30 psi for 10–50 ms). The pipette was kept in place for at least 30 s to limit tracer reflux out of the injection site. After surgery, buprenorphine HCl (0.03 mg/kg) was injected subcutaneously for pain relief during recovery. For spinal cord injections, an incision was made to expose the second cervical vertebral body and a laminectomy was performed to expose the spinal cord; injections were made ~0.8 mm deep and ~0.5 mm left of the midline. In the case of intracranial injections (into the striatum or cortex), an incision was made in the scalp, a craniotomy was made, the dura was reflected, and pipettes were advanced to reach the stereotaxic coordinates of the desired target. The anteroposterior/mediolateral stereotaxic coordinates were (in millimeters relative to bregma/midline): −1.5/3.5 for striatal injections and 1.0/2.0 for intracortical injections. For striatal injections, the pipette was advanced in a dorsolateral-to-ventromedial direction through the posterolateral parietal cortex (angled 18° off the sagittal axis and 52° off the horizontal axis), penetrating to a depth of 3.5 mm from the surface of the brain. For intracortical injections, the pipette was advanced 0.75 mm perpendicular to the surface of the brain.

Slice Preparation

Brain slices were prepared as described (Anderson et al. 2010) at *postnatal days 22–28* (i.e., 1–7 days after bead injections). Coronal slices (coronal slice angle tilted rostrally 10–15°; 300 μm thick) containing primary motor (M1) were made by vibratome sectioning the brain (HM 650 V, Microm International GmbH, Germany) in chilled cutting solution [composed of (in mM): 110 choline chloride, 25 $NaHCO_3$, 25 D-glucose, 11.6 sodium ascorbate, 7 $MgSO_4$, 3.1 sodium pyruvate, 2.5 KCl, 1.25 NaH_2PO_4, and 0.5 $CaCl_2$]. Slices were transferred to artificial cerebrospinal fluid [ACSF; composed of (in mM): 127 NaCl, 25 $NaHCO_3$, 25 D-glucose, 2.5 KCl, 1 $MgCl_2$, 2 $CaCl_2$, and 1.25 NaH_2PO_4, aerated with 95% O_2/5% CO_2] at 34–35°C for 30 min. Slices were subsequently incubated in ACSF at 22°C for at least 1 h prior to electrophysiological recordings.

Electrophysiology

Whole-cell recordings from fluorescently labeled pyramidal neurons were performed as described (Anderson et al. 2010). Briefly, slices were transferred to the recording chamber of an upright microscope (BX51, Olympus, Japan) and held in place with short pieces of flattened gold wire (0.813 mm diameter; Alfa Aesar, Ward Hill, MA). Fluorescently labeled corticospinal neurons were visualized using epifluorescence optics. Pipettes were fabricated from borosilicate capillaries with filaments (G150-F, Warner Instruments, Hamden, CT) using a horizontal puller (P-97, Sutter Instrument, Novato, CA) and filled with intracellular solution composed of (in mM): 128 $KMeSO_3$, 10 HEPES, 1 EGTA, 4 $MgCl_2$, 4 ATP, 0.4 GTP, 10 phosphocreatine, 3 ascorbate, and 0.05 Alexa-594 or -488 (Molecular Probes, Eugene, OR), pH 7.3. EGTA was included both to facilitate seal formation and to reduce cytosolic calcium elevations induced by the various stimulus protocols used in these studies. ACSF was used as the extracellular recording solution. Slices were used up to 10 h after preparation. Recordings were performed at 22°C or 34°C as noted. The ACSF was refreshed every 3 h at 22°C and every 2 h at 34°C. The recording temperature was controlled by an inline heating system (TC-324B, Warner Instruments). Recordings were targeted to neurons 60–100 μm deep in the slice.

Pipette capacitance was compensated; series resistance was monitored but not compensated and required to be <30 MΩ for inclusion in the data set. Current-clamp recordings were bridge balanced. Current was injected as needed to maintain the membrane potential near -70 mV during stimulus protocols (i.e., within the activation range of I_h at baseline). No synaptic blockers were present for current-clamp recordings. Recordings were filtered at 4 kHz and digitized at 10 kHz. Membrane potential values were not corrected for a calculated liquid junction potential of 10 mV (22°C) or 11 mV (34°C).

Voltage sag was measured from a membrane potential of -70 mV by presenting two hyperpolarizing current steps (-100 and -50 pA, 500 ms). Percentage voltage sag was calculated from the peak voltage (V_{peak}) and steady-state voltage ($V_{steady\text{-}state}$), as $100 \times (V_{peak} - V_{steady\text{-}state})/V_{peak}$. The values obtained for the two steps were averaged.

Chirp stimuli (adapted from Shin et al. 2008) were adjusted to produce an ~5-mV response at the maximum frequency of 20 Hz. Responses to chirp stimuli were analyzed to obtain impedance amplitude profiles (ZAPs). Resonant frequencies were determined from ZAPs as the peak (over 0.5–20 Hz) in the frequency domain (boxcar smoothed with a 0.75-Hz window). Synaptic waveforms [α synapses, α-excitatory postsynaptic potentials (αEPSPs)] used to create artificial EPSPs were defined by an α function with a 5-ms time constant; these were scaled in amplitude to give ~5-mV responses to the first pulse.

Voltage-clamp mode recordings of hyperpolarization-activated, cyclic nucleotide-gated cation (HCN) currents were performed in the presence of (in μM): 0.75 TTX (Sigma-Aldrich, St. Louis, MO), 10 XE 991 (M-current blocker; Tocris Bioscience, Ellisville, MO), 10 2,3-dihydroxy-6-nitro-7-sulfamoyl-benzo[f]quinoxaline-2,3-dione (Tocris Bioscience), 10 gabazine (Tocris Bioscience), 5 3-[(±)-2-carboxypiperazin-4-yl]-propyl-1-phosphonic acid (Tocris Bioscience), and 3 mM tetraethylammonium chloride (Sigma-Aldrich), and the intracellular solution contained (in mM): 128 $CsMeSO_3$, 10 HEPES, 1 EGTA, 4 $MgCl_2$, 4 ATP, 0.4 GTP, 10 phosphocreatine, 3 ascorbate, 0.5 QX-314, and 0.05 Alexa-594 or -488 hydrazide (Molecular Probes), pH 7.3. Membrane potential values were not corrected for a calculated liquid junction potential of 11 mV (34°C).

Glutamate Uncaging and Dendritic Mapping

Glutamate uncaging and laser-scanning photostimulation (LSPS) were performed as described previously (Anderson et al. 2010; Shepherd 2011; Weiler et al. 2008), using an UV laser (355 nm; DPSS Lasers, Santa Clara, CA). Ephus software was used for hardware control and data acquisition (http://www.ephus.org) (Suter et al. 2010). Caged glutamate [0.2 mM; 4-methoxy-7-nitroindolinyl-caged-L-glutamate (MNI-glutamate), Tocris Bioscience] was added to the bath solution. For experiments involving repetitive stimulation at a single site, a location was found in layer 2/3, which elicited similar amplitude EPSPs in the two simultaneously recorded neurons; care was taken to avoid sites resulting in any direct stimulation of their dendrites. Such sites were readily detected based on the characteristic waveform properties of direct dendritic responses, including much faster response latencies (<5 ms) compared with synaptic inputs (Schubert et al. 2001). For two-site photostimulation, software tools were implemented to allow the UV laser power to be adjusted independently at each site to produce EPSPs of similar amplitude (~10–15 mV) in both of the recorded neurons.

For dendritic mapping experiments, after establishing a whole-cell recording on a neuron in a brain slice, a low-magnification image of the slice was captured, and a stimulus grid (8×24, 50 μm spacing) was aligned vertically to the pia and horizontally to the soma. Caged glutamate (MNI-glutamate, Tocris Bioscience) was added to the bath solution (0.2 mM). TTX (0.5 μM) was added to eliminate inputs from presynaptic neurons. The power of the UV laser was set to 20 mW in the specimen plane. During mapping, stimulus sites were visited at 1 Hz in a nonraster pattern, which avoided the vicinity of recently stimulated sites (Shepherd et al. 2003). Responses were recorded in current clamp and analyzed offline to determine the mean depolarization over a 0.5-s poststimulus window.

For optogenetic experiments, layer 2/3 pyramidal neurons were selectively transfected by in utero electroporation (IUEP) of plasmids encoding channelrhodopsin-2 (ChR2) fused with a fluorescent protein (Venus), using methods described previously (Anderson et al. 2010; Petreanu et al. 2007; Wood et al. 2009). Coronal brain slices were prepared from mice (age 23–28 days) as described above. To excite ChR2, the same UV laser as for LSPS was used. Because of variability, both in transfection efficiency (i.e., number of ChR2-expressing neurons/animal) and in ChR2 expression levels (i.e., number of ChR2 molecules/transfected neuron), for each slice, we standardized the stimulation intensity by setting the laser power to give one or more action potentials (APs) for an interstimulus interval (ISI) of 25 ms.

Pharmacology

I_h was blocked using low concentrations of the irreversible HCN channel blocker, ZD7288 (Tocris Bioscience). A 25-mM stock solution was made in water, aliquoted, and stored at -20°C. Aliquots were diluted in ACSF for experiments to a final concentration of 25 μM or 10 μM. Cirazoline HCl (Tocris Bioscience) and guanfacine HCl (Tocris Bioscience) were used as α1- and α2-adrenergic agonists, respectively. Stock solutions of cirazoline (1 mM) and guanfacine (40 mM) were made in water, aliquoted, and stored at -20°C. Stock solutions of MNI-caged glutamate (50 mM in water) were prepared at room temperature (to avoid precipitation) with sonication, aliquoted, and stored at -20°C.

Cell Dissociation and Fluorescence-Activated Cell Sorting

Fluorescence-activated cell sorting (FACS) was used to purify fluorescent bead-labeled neurons (Özdinler and Macklis 2006). FACS enables high-purity isolation of cortical neurons, comparable with methods based on manual sorting (Okaty et al. 2011a, b). Coronal slices were prepared as described above. Immediately following slicing, six to eight slices containing motor cortex and adjacent portions of somatosensory cortex were microdissected in cold choline solution, yielding a collection of cortical microslices containing the bead-labeled neurons. These were cut into smaller sections, stored temporarily in ACSF at 34°C, and digested in papain solution (Worthington Biochemical, Lakewood, NJ) at 37°C for 30 min; the digestion was terminated using an ovomucoid stop solution

(Sigma-Aldrich). Cortical neurons were dissociated by trituration using a series of Pasteur pipettes decreasing in tip diameter. Dissociated cells were filtered through nylon mesh (BD Biosciences, San Jose, CA), centrifuged (1,500 rpm, 10 min), and resuspended in Opti-MEM (Invitrogen, Carlsbad, CA) with 1 μg/ml 4′6-diamidino-2-phenylindole (DAPI) to label dead neurons. A high-speed multilaser droplet cell sorter (MoFlo, DakoCytomation, Carpinteria, CA) was used to isolate DAPI-negative, bead-labeled neurons, which were pooled into one sample/animal (corticospinal neurons: ~2,000 cells/animal, three animals; corticocortical: ~2,400 cells/animal, five animals; corticostriatal: ~1,500 cells/animal, three animals). Cells were stored at −80°C until RNA extraction and cDNA synthesis.

RNA Isolation and Real-Time PCR Quantification

Total RNA was isolated from FACS-isolated cells using TRIzol (Invitrogen). RNA samples were treated with DNase I (Ambion, Austin, TX) to eliminate genomic DNA contamination, and cDNA was synthesized using qScript cDNA SuperMix (Quanta BioSciences, Gaithersburg, MD). Real-time PCR was performed using SYBR Green I on a StepOnePlus thermocycler (Applied Biosystems, Foster City, CA). The thermal cycling conditions were comprised of an initial denaturing step at 95°C for 3 min and 40 cycles at 95°C for 15 s, 60°C for 60 s, and 72°C for 30 s. The PCR cycle threshold values were measured within the exponential phase of the PCR reaction using StepOnePlus software (version 2.1, Applied Biosystems). Reactions with any evidence of nonspecificity (i.e., low melting temperatures or multiple peaks in melting-point analysis) were excluded from analysis. A relative quantification method (ΔΔ comparative threshold method) (Schmittgen and Livak 2008) was used to quantify expression levels of HCN1, HCN2, and Trip8b in cortical neurons with GAPDH as an endogenous reference gene. For each sample, reactions for each gene of interest were run in triplicate or quadruplicate. Desalted, intron-spanning primers were custom synthesized (Invitrogen). Primers used for PCR amplification were as follows: HCN1, upper primer GCTGACAGATGGCTCTTACT, lower primer GAAATTGTCCACCGAAAGGG; HCN2, upper primer CCGAGAGCATGACAGACATC, lower primer CCGGTGTTCATAGTAATCGTGG; Trip8b, upper primer CCCCAAACCAAAGCCAAGAAA, lower primer GGTCACCGTGAAACTTGACAT; GAPDH, upper primer TCAACAGCAACTCCCACTCT, lower primer GGTCCAGGGTTTCTTACTCCTT.

No-template and no-RT control assays produced negligible signals, suggesting that primer-dimer formation and genomic DNA contamination effects were small. The mRNA levels in each subgroup of samples were calculated as fold differences relative to whole brain. Data were presented as the median fold difference and the median experimental error (SD) across samples (Bookout et al. 2006). The rank-sum test was used for statistical analysis. Differences between the cell groups were considered significant at confidence levels of 95% ($P < 0.05$).

Statistical analysis. Data analysis was performed offline using MATLAB routines (MathWorks, Natick, MA). Group comparisons were tested using a one-way ANOVA followed by a Student's *t*-test (for normally distributed data) or rank-sum test (for non-

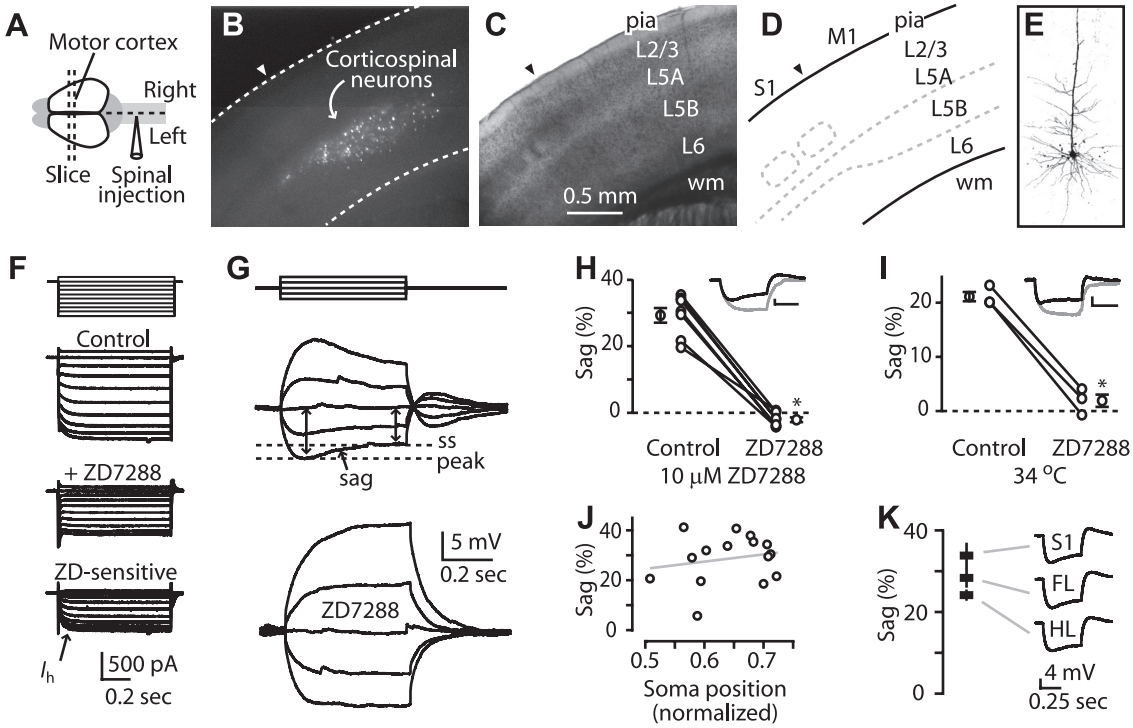

Fig. 1. Corticospinal neurons express high levels of hyperpolarization-activated current (I_h). *A*: injection of fluorescent beads into the cervical spinal cord resulted in retrograde labeling of neurons (*B*) in the contralateral motor cortex. *C*: bright-field image and (*D*) diagram showing cortical layers (L) in motor cortex (wm, white matter; M1, motor cortex; S1, somatosensory cortex). Arrowheads, border between somatosensory cortex (to the *left*) and M1 (to the *right*). *E*: 2-photon image of a biocytin-filled corticospinal neuron in the motor cortex. *F*: voltage-clamp mode recording (voltage steps: multiples of ±10 mV, holding potential −50 mV) from a corticospinal neuron eliciting currents before (Control) and after (+ZD7288) application of ZD7288 (25 μM; 34°C). Current sensitive to ZD7288 (ZD; bottom) represents I_h. *G*: current-clamp recording from a corticospinal neuron showing sag of the membrane potential to a steady-state (ss) level and sensitivity to the I_h blocker ZD7288 (25 μM; current steps: multiples of ±50 pA; 22°C). *H*: ZD7288 sensitivity at 10 μM. Data points for individual neurons are connected by lines, flanked by group means ($n = 7$; bars: ±SE, $^*P < 0.05$, paired *t*-test; 22°C). *I*: sag and sensitivity to ZD7288 measured at 34°C, 25 μM ZD7288 ($n = 3$; $^*P < 0.05$, paired *t*-test). *J*: sag was independent of somatic sublayer location (normalized distance: pia = 0; white matter = 1; line, linear regression; 22°C). *K*: average (±SE) sag for corticospinal neurons in forelimb (FL; $n = 49$) and hindlimb (HL; $n = 10$) regions of the motor cortex and in somatosensory cortex ($n = 10$).

normally distributed data), as indicated. Error bars in plots represent SE.

RESULTS

Corticospinal Neurons Express High Levels of I_h

We fluorescently labeled corticospinal neurons by injecting retrograde tracers in the cervical spinal cord (Fig. 1*A*) and prepared coronal brain slices containing the contralateral motor cortex. Labeled neurons were distributed over the full thickness of layer 5B (Fig. 1, *B–E*). Labeled neurons were targeted for whole-cell recordings with patch electrodes. In voltage-clamp mode, large currents (up to 750 pA, holding potential, $V_{hold} = -50$ mV) were activated by hyperpolarizing voltage steps, and these were sensitive to the I_h antagonist ZD7288 (25 μM; Fig. 1*F*) (Harris and Constanti 1995), indicative of I_h expression in these neurons. Due to the limitations of voltage-clamp mode measurements in these large pyramidal neurons (Williams and Mitchell 2008), subsequent experiments evaluating I_h were carried out in current clamp.

Responses of corticospinal neurons to families of current steps revealed prominent "sag" of the membrane potential (Fig. 1*G*). Sag is characteristic of I_h but can be generated by other voltage-dependent conductances (Stafstrom et al. 1982). However, bath application of ZD7288 (25 μM) eliminated sag, indicating its I_h dependence in these neurons (Fig. 1*G*). Lower concentrations of ZD7288 (10 μM) also eliminated sag (Fig. 1*H*). Experiments at 34°C gave similar results (Fig. 1*I*), and ZD7288 also hyperpolarized the resting membrane potential (by -10 ± 3 mV; mean $\pm$ SD, $n = 7$) and increased the input resistance (by 90 ± 24 MΩ; mean $\pm$ SD, $n = 7$), consistent with the blockade of I_h (Biel et al. 2009).

Although corticospinal neurons are restricted to layer 5B, this is a thick layer in mouse motor cortex (Yu et al. 2008), and local circuit properties vary by sublayer (Anderson et al. 2010). However, sag did not vary among corticospinal neurons as a function of sublayer location (Fig. 1*J*). Because other non-I_h-related intrinsic properties (involved in repetitive firing behavior) have been shown to vary for pyramidal tract (PT)-type neurons located in different cortical areas (motor vs. somatosensory) (Miller et al. 2008), we also explored the possibility that sag varied for corticospinal neurons located in different areas. However, sag was similar for corticospinal neurons located in the forelimb and hindlimb representation areas of motor cortex and in somatosensory cortex (Fig. 1*K*). Thus high I_h expression was a general property of the corticospinal neurons recorded here.

Callosally Projecting Corticostriatal and Corticocortical Neurons Express Relatively Low Levels of I_h

High I_h expression in corticospinal neurons could be either a layer-specific property of layer 5B pyramidal neurons (Nicoll et al. 1993; Spain 1994; Spain et al. 1987; Williams and Stuart 2000) or a projection class-specific property of corticospinal neurons. To investigate this, we examined other types of projection neurons in motor cortex. To label callosally projecting ("crossed") corticostriatal neurons, we injected retrograde tracer into the dorsolateral striatum (Fig. 2*A*) of the contralateral hemisphere. Labeled, crossed corticostriatal neurons were distributed in layers 5A and 5B (Fig. 2*A*). Crossed corticostriatal neurons are intratelencephalic (IT)-type projection neurons, extending axons both to the ipsilateral cortex and striatum and to the contralateral striatum, with possible collaterals to the contralateral cortex; their projection pattern is distinct from that of the PT-type neurons (exemplified by corticospinal neurons), which project to the striatum

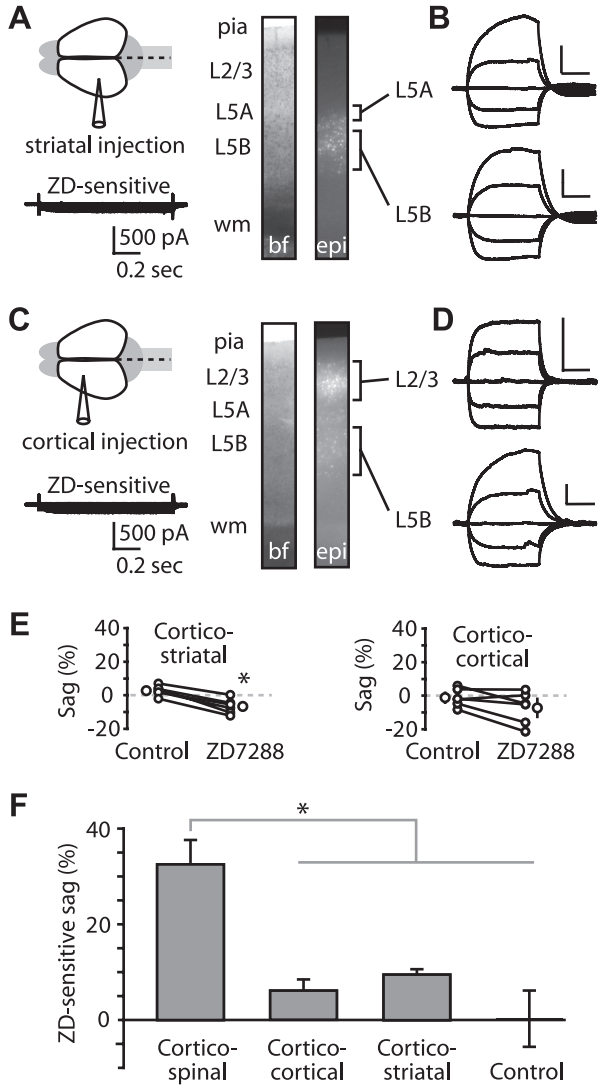

Fig. 2. Crossed corticostriatal and corticocortical neurons express low levels of I_h. *A*: tracer injection into the contralateral dorsolateral striatum resulted in retrograde labeling of crossed corticostriatal neurons in motor cortex, distributed in layers 5A and 5B (images: bf, bright field; epi, epifluorescence). *Bottom*: ZD7288-sensitive current from a recording in voltage-clamp mode (voltage steps -80 to $+10$ mV in 10-mV increments; holding potential -50 mV; 34°C) of a layer 5A corticostriatal neuron. *B*: current-clamp recordings from labeled corticostriatal neurons in layers 5A and 5B. Scale bars: 10 mV, 0.2 s (applies throughout). *C*: injection into the contralateral motor cortex labeled callosally projecting corticocortical neurons in motor cortex, distributed across multiple superficial and deep layers. *Bottom*: ZD7288-sensitive current from a voltage-clamp mode recording (voltage steps same as *A*) of a layer 5B corticocortical neuron. *D*: recordings from layers 2/3 and 5 corticocortical neurons. *E*: effect of ZD7288 on sag in corticostriatal ($n = 6$; $^*P < 0.05$, paired *t*-test; 22°C) and corticocortical neurons ($n = 6$; $P > 0.05$, paired *t*-test; 22°C). *F*: ZD7288-induced change in sag for corticospinal ($n = 7$), corticocortical ($n = 6$), and corticostriatal ($n = 6$) neurons ($^*P < 0.05$, *t*-test, corticospinal vs. other groups). Control neurons ($n = 3$) are time-control recordings from corticospinal neurons with no drug application to test for I_h changes over the duration of the recording.

only ipsilaterally (Catsman-Berrevoets et al. 1980; Reiner 2010; Reiner et al. 2010). Corticostriatal neurons produced small (~150 pA) hyperpolarization-activated currents sensitive to ZD7288 (Fig. 2*A*). Sag was small in corticostriatal neurons, both in layers 5A and 5B (Fig. 2*B*).

Corticocortical neurons are another example of IT-type neurons (Reiner 2010). Therefore, if low I_h expression is a general property of IT-type neurons, one would expect to find low I_h expression in corticocortical neurons. Injection of a retrograde tracer into the motor cortex of the contralateral hemisphere resulted in labeling of callosally projecting corticocortical neurons, distributed in layers 2/3 and 5B (Fig. 2*C*). These cells also produced small (~150 pA) hyperpolarization-activated currents sensitive to ZD7288 (Fig. 2*C*). Sag was small in corticocortical neurons, both in layers 2/3 and 5B (Fig. 2*D*).

Sag in corticostriatal neurons, although small, was reduced significantly by ZD7288 (Fig. 2, *E* and *F*). The ZD7288-sensitive component in corticostriatal (9.4 ± 1.0%) neurons was significantly smaller than in corticospinal neurons (32.4 ± 5.3%; $P < 0.05$, *t*-test). Similarly, the ZD7288-sensitive sag in corticocortical neurons (6.1 ± 2.4%) was significantly smaller than in corticospinal neurons ($P < 0.05$, *t*-test; Fig. 2, *E* and *F*). In this case, the reduction in sag by ZD7288 did not reach statistical significance (Fig. 2*E*). These data indicate that corticostriatal and corticocortical projection neurons express low levels of I_h.

HCN1 and Trip8b Subunit Expression is High in Corticospinal Compared with Corticostriatal and Corticocortical Neurons

We next investigated the molecular basis for the electrophysiologically and pharmacologically identified differences in I_h by performing FACS and quantitative PCR analysis (FACS-qPCR) on retrogradely labeled neurons of each projection class. Expression levels were quantified for HCN1 and HCN2 genes, the major isoforms expressed in brain (Moosmang et al. 1999; Notomi and Shigemoto 2004; Santoro et al. 2010), and referenced to GAPDH expression levels (Chan et al. 2011). We also probed for Trip8b, a protein involved in trafficking of HCN subunits to dendritic membranes, including establishment of somatodendritic HCN1 channel gradients (Lewis et al. 2009; Lewis et al. 2011; Santoro et al. 2004, 2009).

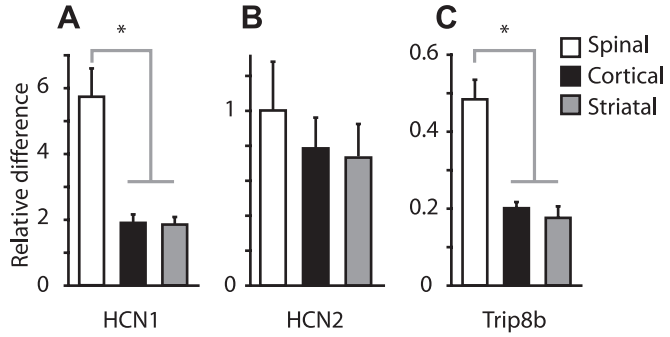

Fig. 3. Hyperpolarization-activated, cyclic nucleotide-gated cation (HCN) channel subunit expression in projection neurons. Fluorescently labeled projection neurons were fluorescence-activated cell sorting purified, and expression levels of HCN1 (*A*), HCN2 (*B*), and Trip8b (*C*) were quantified using quantitative PCR. Expression levels for each gene target are plotted as fold difference relative to whole brain (*$P < 0.05$, rank-sum test). For each sample ($n = 3$ corticospinal-labeled mice; 3 corticostriatal; 5 corticocortical), reactions were run in triplicate or quadruplicate, and the median (and SD) across reactions was calculated. Plots show the median values (and median SD) across samples. For further details, see MATERIALS AND METHODS, *RNA isolation and real-time PCR quantification*.

Expression of HCN1 was higher in corticospinal neurons compared with either corticocortical ($P < 0.05$, Mann-Whitney U test) or corticostriatal neurons ($P < 0.05$) (Fig. 3*A*). HCN1 levels did not differ significantly between corticocortical and corticostriatal neurons ($P > 0.05$; Fig. 3*A*). HCN2 was expressed at similar levels in all three groups ($P > 0.05$; Fig. 3*B*). Expression of Trip8b followed the same pattern as HCN1: high in corticospinal and low in corticostriatal and corticocortical neurons ($P < 0.05$; Fig. 3*C*). The pattern of HCN1 and Trip8b subunit expression in these three projection classes closely resembled that observed physiologically.

I_h Attenuates Responses to Glutamate Uncaging Across Dendrites of Corticospinal Neurons

In cortical pyramidal neurons, functional HCN channels are distributed throughout dendritic arbors, increasing in a graded manner with distance from the soma (Berger et al. 2001; Kole et al. 2006; Lewis et al. 2011; Lorincz et al. 2002; Magee 1998; Stuart and Spruston 1998; Williams and Stuart 2000). To explore the effect of I_h on dendritic responses to glutamate stimulation, we recorded from the soma of neurons (in the presence of 0.5 μM TTX to block presynaptic inputs) and evoked responses at an array of locations across their dendritic arbors using focal glutamate uncaging (Fig. 4*A*). Responses were measured before and after I_h blockade with ZD7288 (Fig. 4*B*). On average, ZD7288 markedly increased the amplitude of responses to glutamate uncaging across the dendritic arbors of corticospinal neurons ($n = 9$; Fig. 4*C*). As shown by plotting the vertical profiles of the average responses (Fig. 4*D*), the largest absolute differences were observed for stimuli around the soma (i.e., in the basal and proximal apical dendritic subarbors; region "c" in Fig. 4, *D, E*), whereas the largest relative differences were observed for stimuli around the apical tuft. We note that although this spatial pattern is consistent with an I_h gradient described previously (Berger et al. 2001; Kole et al. 2006; Lorincz et al. 2002; Magee 1998; Stuart and Spruston 1998; Williams and Stuart 2000), the method used here does not directly demonstrate a gradient of HCN channel density. Instead, responses recorded at the soma represent the cumulative effect of dendritic I_h in filtering signals propagating from the dendritic site of stimulation.

ZD7288 caused negligible differences in the mean responses of corticostriatal neurons ($n = 5$), and no I_h effect was identified in either apical or basal regions of dendritic arbors (Fig. 4, *F–J*). Thus these findings extend the characterization of I_h differences in corticospinal and corticostriatal neurons, showing I_h-dependent attenuation, not only for apical but also and indeed prominently for proximal dendritic responses in corticospinal neurons. One implication of these electroanatomical results is that dendritic arbor morphology is unlikely to account for the electrophysiological differences in I_h, because the dendritic architecture of corticospinal and corticostriatal neurons differs primarily in the apical tuft dendrites and not in the proximal and basal arbors (Gao and Zheng 2004), where the largest (absolute) I_h-dependent responses were observed. In other words, I_h differences cannot be ascribed merely to the presence, in corticospinal neurons only, of a HCN-rich apical

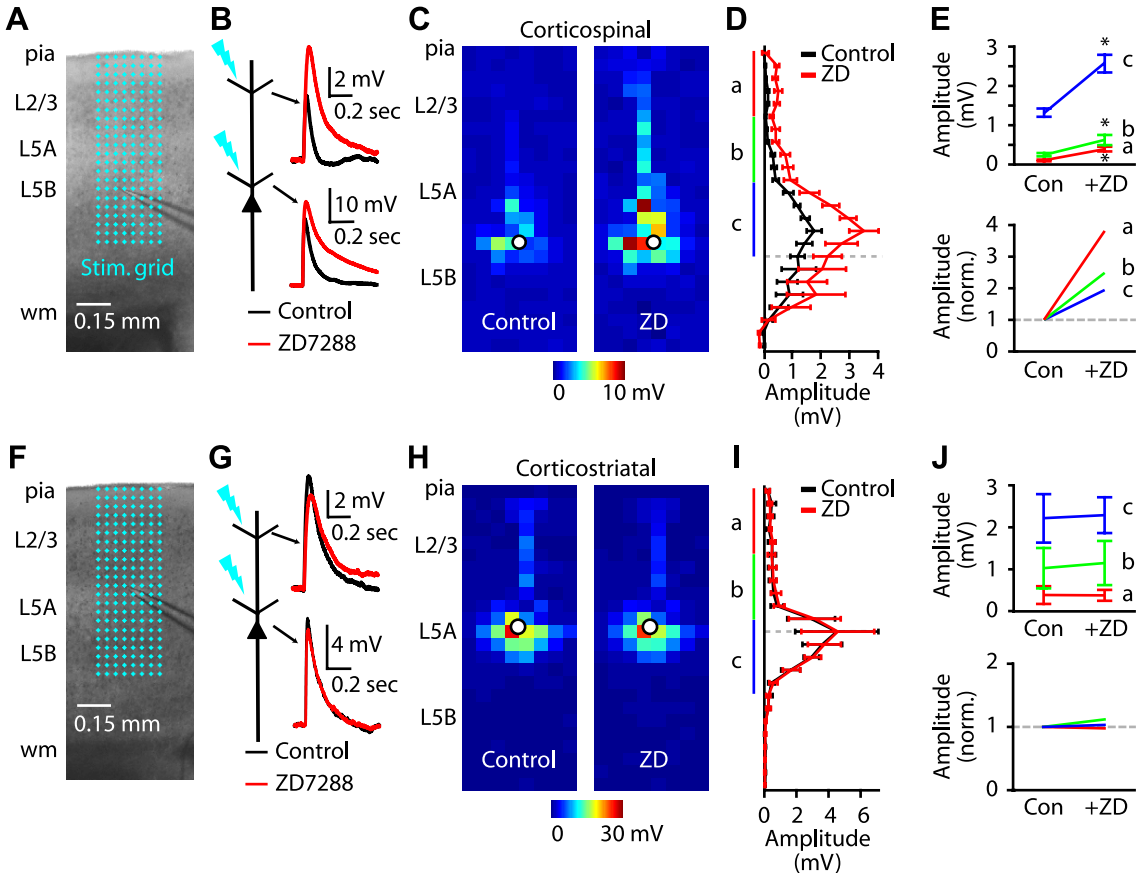

Fig. 4. Optical mapping of the I_h dependence of excitatory responses evoked across dendritic arbors by focal glutamate uncaging. *A*: example (4× bright-field video image) of a corticospinal recording overlaid with the 8 × 24 stimulation grid (50 μm spacing) for dendritic mapping. *B*: example traces of corticospinal responses before and after ZD7288 application, for apical tuft (*top*) and proximal (*bottom*) dendritic locations. *C*: example dendritic map of a corticospinal neuron before (*left*) and after (*right*) application of ZD7288. Each pixel represents the mean amplitude of the response evoked by UV photolysis of MNI-glutamate at that location. *D*: mean (±SE) vertical profile, calculated by projecting each neuron's map to a single vector (by averaging along map rows) and then averaging across all corticospinal neurons (n = 9). Dashed line, mean soma position; *a*: distal apical; *b*: proximal apical; *c*: basal. *E*: absolute (*top*) and normalized (*bottom*) magnitude of ZD7288 sensitivity for distal apical (*a*), proximal apical (*b*), and basal (*c*) dendrites (*$P < 0.05$, paired t-test). Con, control. *F*: example of a corticostriatal recording, as in *A*. *G*: corticostriatal traces, as in *B*. *H*: example dendritic map of a corticostriatal neuron before (*left*) and after (*right*) application of ZD7288. *I*: mean profile for corticostriatal neurons (n = 5). *J*: region-of-interest analyses, as in *E*.

tuft, because HCN channels appear to be abundant in the basal and proximal apical dendrites as well.

Sag and Resonance in Corticospinal Neurons are I_h Dependent and Projection Specific

To explore the relationship between I_h expression levels and intrinsic properties of projectionally defined classes of motor cortex pyramidal neurons, we undertook additional, functional characterizations at 34°C. First, we measured sag for the different classes as a function of the precise position of the soma along the radial axis of the cortex (Fig. 5*A*). Analysis of group data in terms of cell class showed that corticospinal neurons expressed significantly more sag than other pyramidal cell classes (Fig. 5*B*), corroborating and extending similar data shown above (Figs. 1 and 2). Amplitude of voltage sag was also significantly larger ($P < 0.05$, one-way ANOVA) in corticospinal neurons (0.7 ± 0.1 mV, n = 10) compared with corticostriatal (−0.3 ± 0.2 mV, n = 20) and corticocortical (−0.1 ± 0.1 mV, n = 12) neurons. Again, ZD7288 eliminated sag in corticospinal neurons (Fig. 5, *A* and *B*).

Because I_h can strongly influence neuronal resonance (Hutcheon and Yarom 2000; Narayanan and Johnston 2007; Shin et al. 2008), we delivered subthreshold chirp stimuli (frequency-swept sinusoids ranging linearly from 0 to 20 Hz over 20 s) and calculated ZAPs so as to estimate the frequency tuning and resonance properties of these neurons (Fig. 5, *C* and *D*). ZAPs of corticospinal neurons exhibited a broad peak centered at ~4 Hz (Fig. 5, *D* and *E*). In contrast, ZAPs of other types of projection neurons, located in the same or different layers, declined monotonically with frequency (Fig. 5*F*). When I_h in corticospinal neurons was blocked, their ZAPs resembled those of noncorticospinal neuron classes (Fig. 5, *D*–*G*).

Adrenergic Effects in Corticospinal Neurons Depend on I_h

An important aspect of I_h is that it is under potent neuromodulatory control, which can profoundly alter the electrophysiological properties of neurons (Biel et al. 2009). Therefore, we next explored the G-protein-coupled receptor-mediated modulation of I_h, focusing on subthreshold properties of corticospinal and corticostriatal neurons. Given the high I_h expression in corticospinal neurons, we hypothesized that noradrenergic stimulation would be relatively selective for corticospinal over corticostriatal neurons. Because endogenous nor-

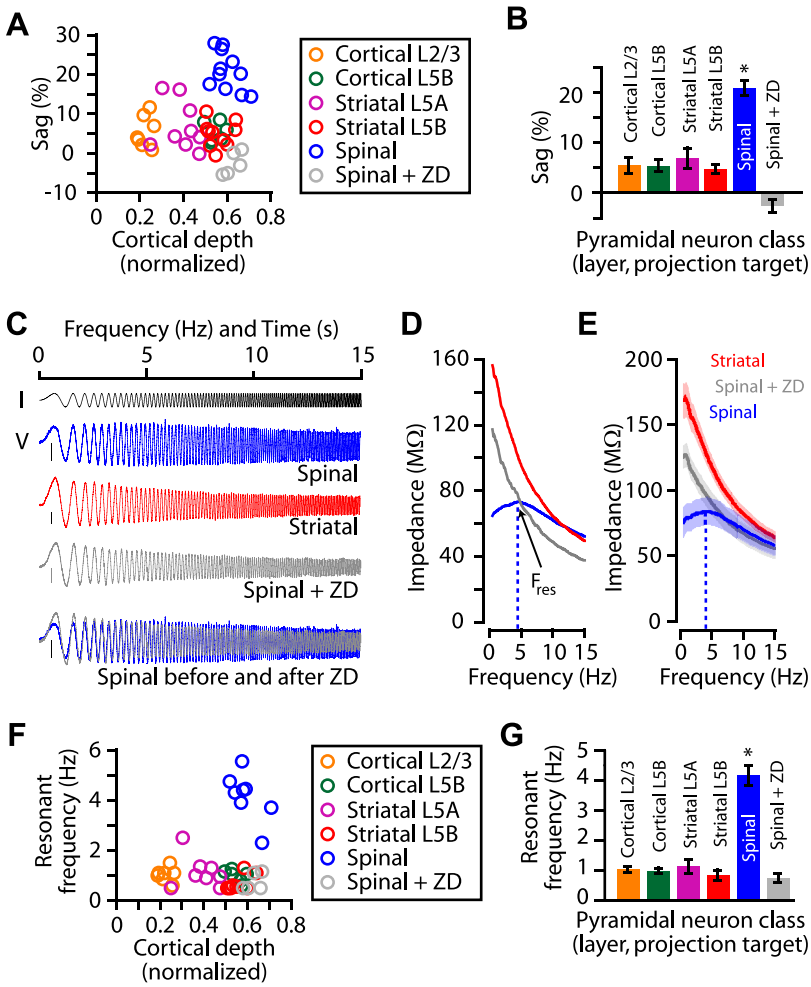

Fig. 5. I_h-dependent sag and resonance across neuronal subclasses. *A*: sag as a function of normalized (pia = 0; white matter = 1) soma location for projection neuron classes (including corticospinal + ZD7288). *B*: mean (±SE) sag amplitude across projection neuron classes (*$P < 0.05$, *t*-test, corticospinal vs. other groups). Cortical layer 2/3 ($n = 7$); cortical layer 5B ($n = 6$); striatal layer 5A ($n = 9$); striatal layer 5B ($n = 11$); spinal ($n = 11$); spinal + ZD7288 ($n = 5$). *C*: chirp current (I) stimulus (black) and examples of chirp voltage (V) responses, recorded from corticospinal (blue) and corticostriatal (red) neurons, and a corticospinal neuron in the presence of ZD7288 (gray). Only the first 15 s of the sweeps are shown. *Bottom*: normalized and overlayed voltage responses of a corticospinal neuron before (blue) and after (gray) ZD7288 treatment. *D*: examples and (*E*) mean (±SE) of impedance amplitude profiles. Red, corticostriatal; blue, corticospinal; gray, corticospinal + ZD7288. F_{res}, resonant frequency (dashed line). *F*: resonant frequencies vs. soma location for projection neuron classes (including corticospinal + ZD7288). *G*: mean (±SE) resonant frequencies across projection neuron classes (*$P <$ 0.05, rank-sum test; corticospinal vs. other groups). Cortical layer 2/3 ($n = 7$); cortical layer 5B ($n = 6$); striatal layer 5A ($n = 8$); striatal layer 5B ($n = 9$); spinal ($n = 8$); spinal + ZD7288 ($n = 5$).

epinephrine would be expected to stimulate α-adrenoreceptors broadly, we used a combination of the α1-adrenergic agonist cirazoline (1 μM) and the α2-adrenergic agonist guanfacine (40 μM). Application of these agonists significantly reduced sag, eliminated resonance, and increased input resistance in corticospinal neurons (Fig. 6*A*), consistent with a functional decrease in I_h. AP properties (threshold, spike frequency adaptation, AP width) were unchanged. In contrast, for corticostriatal neurons, these α-adrenergic agonists did not significantly change sag, resonance, or input resistance (Fig. 6*B*). We then tested the effects of adrenergic agonists while blocking I_h using intracellular ZD7288 (25 μM). Reducing I_h in corticospinal neurons eliminated the effects of cirazoline and guanfacine (Fig. 6*C*), indicating that I_h modulation underlies the observed adrenergic influence on corticospinal neurons.

Effect of I_h *on Synaptic Integration of Local Inputs to Corticospinal Neurons*

In the ensuing experiments in this study, we examined the influence of corticospinal-specific I_h expression on synaptic integration. First, we recorded from corticospinal or corticostriatal neurons and quantified the efficacy of temporal summation by delivering 20 Hz trains of five EPSP-like waveforms (αEPSPs) injected at the soma via the patch pipette (Fig. 7*A*). We chose this stimulus frequency, because similar frequencies can modulate spiking in layer 5 pyramidal neurons (van Aerde et al. 2009). At this frequency, temporal summation of αEPSPs was minimal in corticospinal neurons but robust in corticostriatal neurons and in corticospinal neurons recorded with ZD7288 in the bath solution (Fig. 7, *A* and *B*). These data indicate that I_h, activated by somatic current injection, strongly attenuates the summation of αEPSPs in corticospinal neurons.

Although injection of αEPSP waveforms via a somatic patch pipette is likely a good indicator (at least qualitatively) of how actual synaptic inputs are integrated, we were interested in testing the effect of I_h in attenuating EPSPs arising from specific populations of presynaptic pyramidal neurons in the local circuit. Because layer 2/3 is a prominent source of interlaminar excitatory input to corticospinal neurons (in layer 5B) and to corticostriatal neurons (in layer 5A) (Anderson et al. 2010), we focused on these microcircuits in the following experiments. We dual injected retrograde tracers of different colors into the contralateral striatum and spinal cord of mice. After a delay to allow retrograde labeling, we prepared brain slices containing motor cortex and recorded simultaneously from pairs of identified projection neurons: an upper-5B corticospinal neuron and a lower-5A corticostriatal neuron (Fig. 8*A*). We used focal glutamate uncaging to evoke APs in neurons at a single presynaptic site in layer 2/3 (Fig. 8*A*) and presented trains of four photostimuli at 20 Hz (Fig. 8*B*). In both postsynaptic cell types, responses declined during repetitive stimulation. Some portion of this decline represents presynaptic

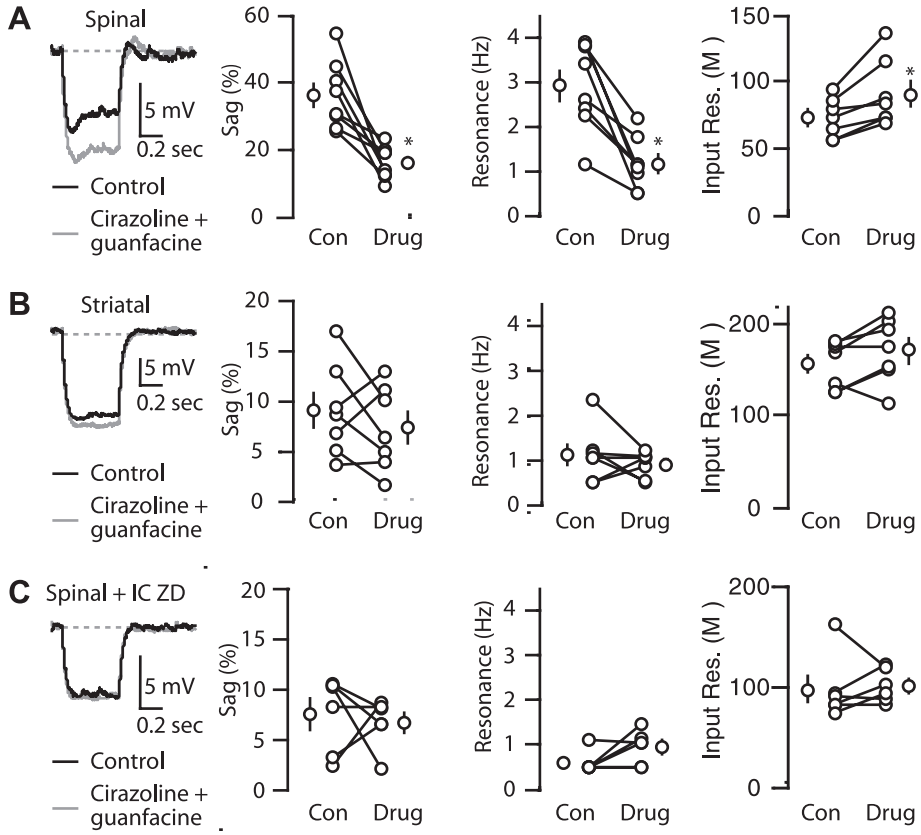

Fig. 6. Adrenergic modulation of I_h-mediated effects in corticospinal neurons. Voltage traces (−100 pA, 0.5 s step; −70 holding, 34°C) of a (*A*) corticospinal neuron, (*B*) corticostriatal neuron, and (*C*) corticospinal neuron recorded with intracellular (IC) ZD7288 before and after combined treatment with the α1-adrenergic agonist cirazoline (1 μM) and the α2-adrenergic agonist guanfacine (40 μM). Plots to the right of the traces show the mean (±SE) effect of adrenergic agonists on voltage sag and resonance corticospinal neurons ($n = 7$), corticostriatal neurons ($n = 7$), corticospinal neurons recorded with intracellular ZD7288 ($n = 6$; $^*P < 0.05$, pair-wise *t*-test).

effects, including caged compound depletion and glutamate receptor desensitization. However, such effects would be expected to be essentially identical for the two simultaneously recorded postsynaptic neurons. Therefore, this approach allowed us to quantify the relative differences in responses. On average, temporal summation of layer 2/3 excitatory synaptic inputs was smaller in corticospinal neurons compared with corticostriatal neurons, a difference that increased during the train (Fig. 8*C*). Normalizing these data to the amplitude of the corticospinal response on a pulse-by-pulse basis showed a steady increase in corticostriatal response relative to the corticospinal response (Fig. 8*D*), similar to the results with the αEPSPs (Fig. 7*B*). We also recorded from pairs of corticospinal neurons, with ZD7288 in the intracellular pipette solution for one of the neurons (Fig. 8*E*). In this case, the block of I_h resulted in stronger summation, similar to corticostriatal neurons (Fig. 8, *F* and *G*). These results demonstrate that synaptic integration by an identified postsynaptic projection neuron in a specific intracortical microcircuit—the excitatory layer 2/3 → corticospinal pathway—is subject to the attenuating effect exerted by I_h.

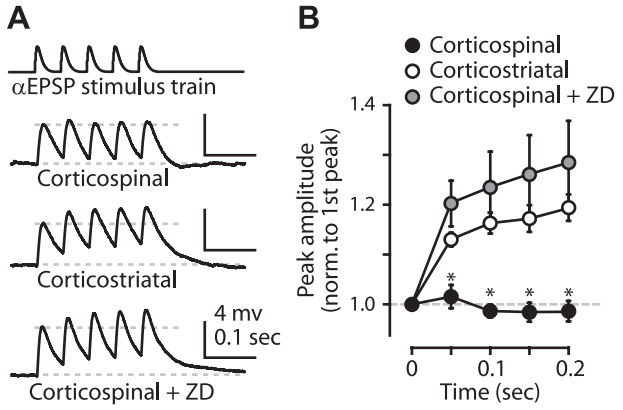

Fig. 7. I_h reduces the temporal summation of artificial α-excitatory postsynaptic potentials (αEPSPs) in corticospinal neurons. *A*: responses to a 20-Hz train of 5 EPSP-like waveforms (*top*) recorded in a corticospinal neuron, corticostriatal neuron, and corticospinal neuron treated with ZD7288. Dotted gray lines indicate the baseline of the recording and the amplitude of first response. *B*: mean (±SE) values of peak responses in the trains of EPSPs, normalized to first peak ($^*P < 0.05$, *t*-test; $n = 5$ corticospinal, 6 corticostriatal, and 7 corticospinal plus ZD7288).

We next explored more distributed effects of I_h on EPSP summation in corticospinal neurons by developing a paradigm for stimulating distinct sets of presynaptic neurons in layer 2/3, separated both spatially and temporally (Fig. 9). We photostimulated two presynaptic sites in layer 2/3, each located ~0.5 mm to either side of the soma (Fig. 9, *A* and *B*), at a range of ISIs [time lag (Δt) = 10–200 ms], while recording EPSPs in a single projection neuron. Compared with corticospinal neurons, summation of closely timed EPSPs was significantly greater in corticostriatal neurons and in corticospinal neurons with ZD7288 in the intracellular pipette solution (Fig. 9, *C* and *D*). This difference was greatest for Δt over the range of 25–75 ms (Fig. 9*D*). These data imply that the presence of I_h in corticospinal neurons shortens the time course of synaptic input and narrows the temporal window for summation of excitatory synaptic inputs.

I_h Regulates Corticospinal Output from Motor Cortical Circuits

Next, we sought to determine the importance of I_h in converting local excitatory inputs into corticospinal output to the spinal cord, i.e., AP generation. We aimed to apply an in

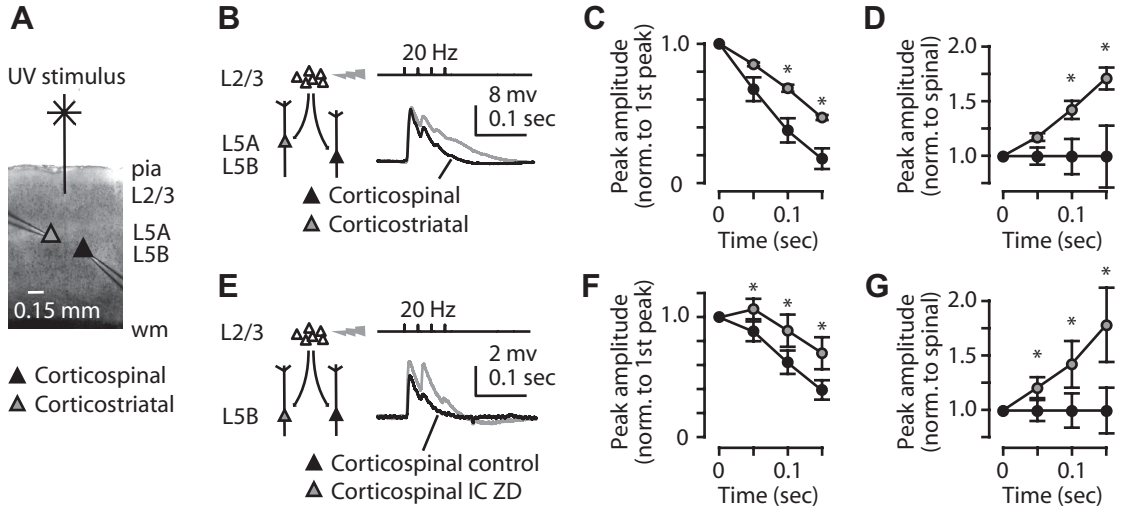

Fig. 8. I_h reduces the temporal summation of excitatory inputs evoked by repetitive stimulation of the same set of layer 2/3 pyramidal neurons. *A*: bright-field image displaying the configuration of pair recording in motor cortex (scale bar, 150 μm). *B*: schematic depicting stimulation by focal UV photolysis of caged glutamate of a common presynaptic site for simultaneously recorded corticospinal and corticostriatal neurons. Traces show the corticostriatal (gray) and corticospinal (black) neurons' responses to a train of 4 stimuli at 20 Hz. *C*: mean (±SE) peak responses of corticospinal (black) and corticostriatal (gray) neurons, normalized to the first peak (*$P < 0.05$, paired *t*-test; $n = 4$ pair recordings). *D*: same data as in *C* but normalized to the mean value of the corticospinal peak response for each EPSP. *E*: same as in *B* but for a simultaneous pair of corticospinal neurons, 1 of which was patched with ZD7288 in the intracellular solution (gray). *F*: mean (±SE) peak responses, normalized to the first peak (*$P < 0.05$, paired *t*-test; $n = 7$ pair recordings). Symbols defined in E. *G*: same data as in *F* but normalized to the mean value of the corticospinal peak response for each EPSP.

vitro paradigm for generating rapid barrages of spatially distributed synaptic inputs to cortical neurons (Boucsein et al. 2005; Losonczy et al. 2010). However, rapid multisite glutamate uncaging proved unsuited for this purpose, due to direct stimulation of the recorded neuron's dendrites by free glutamate (data not shown). Instead, we transfected ChR2 into layer 2/3 pyramidal neurons by IUEP (Fig. 10*A*). Thus in slices containing motor cortex and retrogradely labeled corticospinal neurons, we had optogenetic control of presynaptic layer 2/3 cell bodies and axons. In this case, because only layer 2/3 neurons expressed ChR2, our photostimulation paradigm allowed us to selectively activate layer 2/3 inputs while avoiding direct stimulation of the recorded neuron's dendrites. To emulate rapid activity in multiple convergent inputs, we stimulated ChR2-expressing layer 2/3 cell bodies and axons in rapid succession across an array of locations at high frequencies (8 × 16 stimulation grid, 65 μm spacing; Fig. 10*B*) in a sequence designed to maximize the spatiotemporal separation of sites ("pseudorandom" order). This stimulation paradigm was used to generate rapid and sustained barrages of EPSPs in corticospinal neurons and APs (Fig. 10*C*).

We were especially interested in evaluating ISIs corresponding to the maximal differences in coincidence detection windows (25 and 50 ms). The number of APs generated in corticospinal neurons during spatially distributed, high-frequency layer 2/3 stimulation increased significantly following blockade of I_h by ZD7288 application, an effect observed both at 40 Hz (25 ms ISI; Fig. 11, *A* and *B*) and 20 Hz (50 ms ISI; Fig. 11, *C* and *D*). Corticostriatal neurons differed from corticospinal neurons in two ways: fewer neurons reached firing

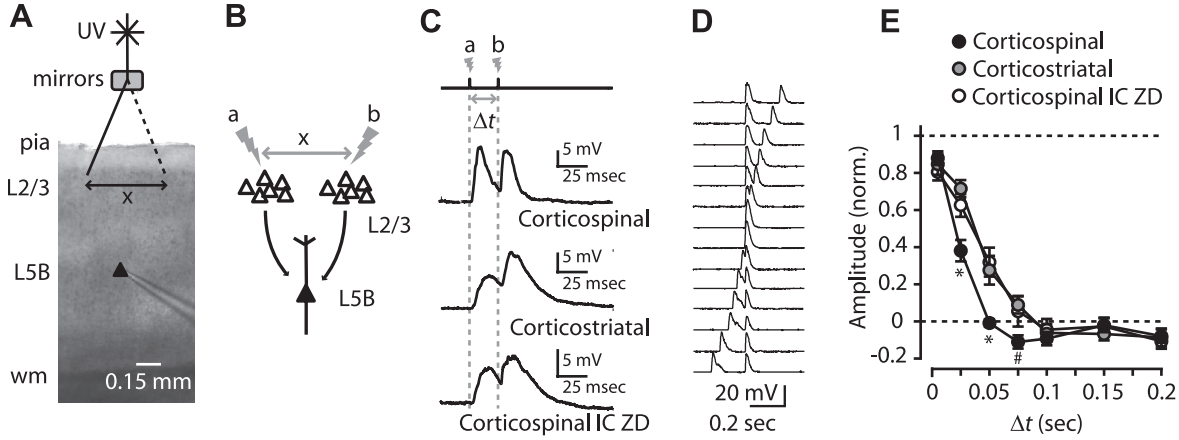

Fig. 9. I_h narrows the coincidence detection time window for EPSPs from 2 spatially distributed sets of layer 2/3 pyramidal neurons. *A*: bright-field (4×) image of slice recording configuration (scale bar, 0.15 mm) depicting UV stimulation [time lag (Δt)] of EPSPs from 2 different layer 2/3 sites separated by ~0.5 mm. *B*: schematic depicting stimulation protocol. *C*: traces show responses of a corticospinal neuron, corticostriatal neuron, and corticospinal neuron recorded with intracellular ZD7288 to stimulation of 2 sites (*a* and *b*) with an interstimulus interval (ISI; Δt) of 50 ms (20 Hz). *D*: example of a family of responses for the stimulation paradigm, recorded from a corticospinal neuron. *E*: mean (±SE) amplitude of peak responses vs. Δt, normalized to maximum depolarization and to minimum depolarization (*$P < 0.05$; #significance between corticospinal and corticostriatal).

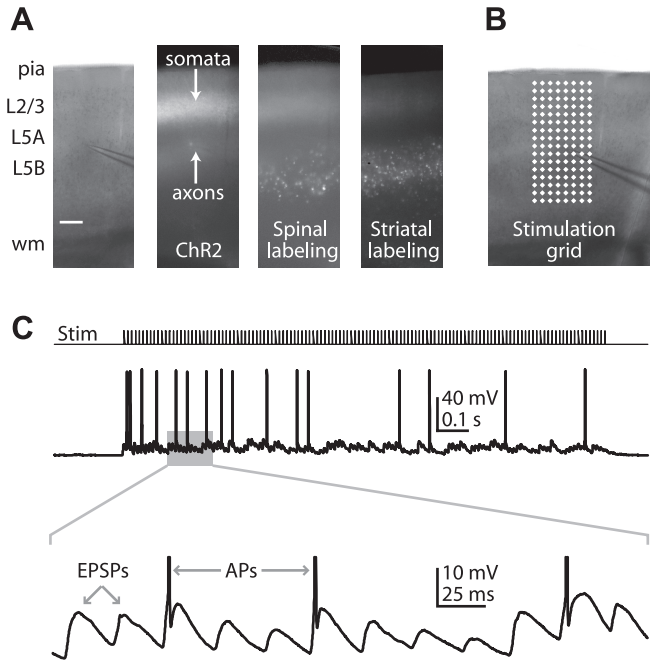

Fig. 10. . Paradigm for rapid photostimulation of layer 2/3 inputs to corticospinal neurons. *A*: images displaying a 4× bright-field example (scale bar, 0.15 mm) of a corticospinal recording (*left*), channelrhodopsin-2 (ChR2) expression (*2nd from left*), corticospinal labeling (*2nd from right*), and corticostriatal labeling (*right*). *B*: stimulation grid. *C*: example of corticospinal action potentials (APs) generated during rapid ChR2 photostimulation (ISI, 25 ms). *Bottom*: expanded view of EPSPs and (truncated) APs.

threshold (five out of 31 neurons), and when they did, on average, they did not fire more APs after ZD7288 treatment at either 25 or 50 ms ISI (Fig. 11).

DISCUSSION

Class-Specific Expression of I_h and of HCN1 and Trip8b Subunits in Motor Cortex Projection Neurons

Electrophysiological and pharmacological experiments showed that mouse corticospinal neurons express high levels of I_h, and corticostriatal and corticocortical neurons express low levels of I_h. A similar pattern of projection class specificity was observed in the relative expression levels of HCN1 and Trip8b subunits. Differences were also detected by optically mapping the ZD7288 sensitivity of glutamatergic stimulation across the dendritic arbors of projection neurons. High I_h expression in corticospinal neurons caused greater membrane potential sag in response to steps of injected current and resonance at ~4 Hz in response to frequency-swept sinusoidal current injection, compared with corticostriatal and corticocortical neurons. These subthreshold corticospinal-specific properties were sensitive to α-adrenergic agonists.

These results provide further evidence for the idea that class-specific I_h expression in neocortical pyramidal neurons is related primarily to their long-range axonal projections and secondarily to their somatic layer (or sublayer) location (e.g., Brown and Hestrin 2009b; Christophe et al. 2005; Dembrow et al. 2010; Kasper et al. 1994). Corticostriatal and corticocortical neurons, distributed over multiple layers and sublayers, expressed low levels of I_h, whereas corticospinal neurons throughout layer 5B (a thick layer in the motor cortex), expressed high levels of I_h. Therefore, the apparent layer specificity of I_h expression (e.g., high in layer 5B, low in layers 2/3 and 5A) arose from the distinct laminar distributions of different projection neurons. In other words, the high I_h in layer 5B reflects the restriction of corticospinal neurons to this layer; within this layer, however, only corticospinal neurons, and not neighboring corticocortical or corticostriatal neurons, selectively expressed high I_h.

The levels of I_h and HCN subunit expression in corticocortical and corticostriatal neurons, although small compared with corticospinal neurons, were nonzero. Previous studies similarly found high and low I_h expression in corticotectal and corticocortical projection neurons in the visual cortex (Christophe et al. 2005) and low I_h expression in layer 2/3 neurons (Larkum et al. 2007). We expect that I_h is functionally important in these neurons in ways that were not revealed by the experimental paradigms applied here. For example, HCN channels can interact with various other conductances and neuromodulatory mechanisms to produce distinct electrophysiological behaviors (Biel et al. 2009). The function of I_h in these callosal projection neurons remains to be identified.

Our results can also be interpreted in the broader context of two superclasses of projection neurons: IT-type and PT-type neurons (Reiner 2010; Reiner et al. 2010). IT-type neurons—exemplified here by corticocortical and corticostriatal neurons—project their axons to ipsilateral and contralateral cortical and striatal targets but not to brainstem or spinal cord. In contrast, PT-type neurons—exemplified here by corticospinal neurons—project their axons to brainstem or spinal cord targets and also to ipsilateral but not contralateral striatum. Within the striatum, IT-type neurons preferentially feed into the direct pathway, whereas PT-type neurons feed into the indirect pathway (Lei et al. 2004). Differential expression of I_h in IT- and PT-type neurons, as suggested by the present findings, could have important implications for understanding the dynamics of information flow in these motor subsystems. In particular, one interpretation is that the "gain" of the layer 2/3 → corticospinal pathway is reduced by the attenuating effect of I_h compared with the layer 2/3 → corticostriatal pathway, a difference that would increase during barrages of presynaptic activity. Consistent with this possibility was the finding here that synaptic integration in corticospinal but not corticostriatal neurons was strongly I_h dependent (discussed in next section).

A previous study (Christophe et al. 2005) of retrogradely labeled layer 5 pyramidal neurons in mouse visual cortex found greater sag in corticotectal neurons (presumably PT-type) than in corticocortical neurons (IT-type), broadly consistent with the IT/PT pattern observed here. However, in that study, single-cell PCR did not detect any differences in HCN1 and HCN2 expression levels, either within or across cell types. In contrast, a study using FACS of different classes of fluorescent interneurons and RT-qPCR found a correlation between HCN1 transcript level and I_h (Sugino et al. 2006). Furthermore, PCR analysis of HCN subunit expression in prefrontal cortex (PFC) pyramidal neurons suggested high expression of HCN1 and low expression of HCN2 transcripts (Day et al. 2005), matching the electrophysiological profile of the same neurons and the brain distribution of HCN1 and HCN2 subunits (Moosmang et al. 1999). Here, we found a similar pattern (high HCN1 and low HCN2) in all three projection classes; moreover, with

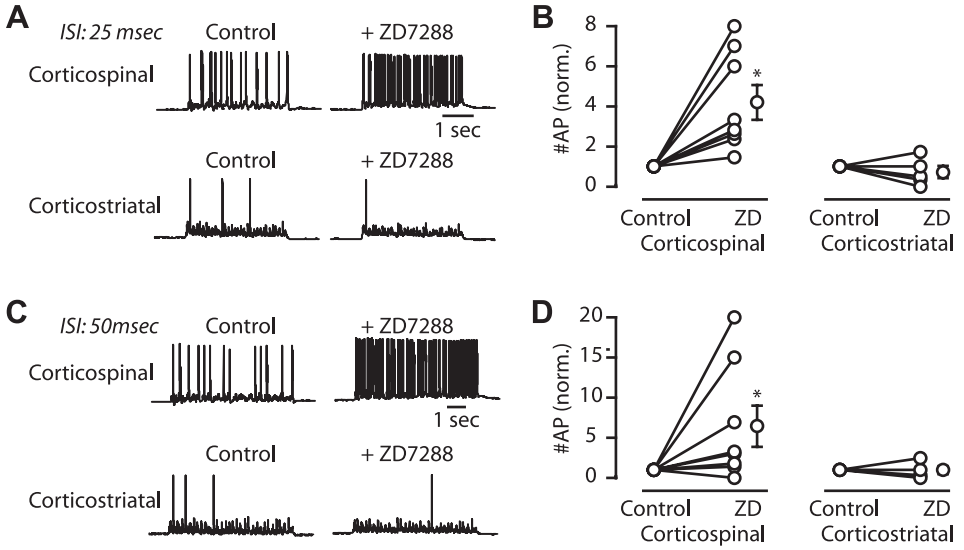

Fig. 11. Reducing I_h increases corticospinal output induced from local excitatory circuits in motor cortex. *A*: examples of corticospinal and corticostriatal neurons' responses to rapid stimulation (34°C; ISI = 25 ms) before (*left*) and after (*right*) treatment with ZD7288. Resting membrane potentials were adjusted to −70 mV by somatic current injection through the patch pipette. *B*: mean (±SE) firing rate induced by rapid stimulation before and after ZD7288, normalized to the pre-ZD7288 value, for corticospinal and corticostriatal neurons (*$P < 0.05$, pair-wise *t*-test). *C* and *D*: same as *A* and *B*, with ISI of 50 ms.

qPCR, we detected differences in HCN1 (and Trip8b) expression between the high-I_h and low-I_h projection classes. Our findings underscore the utility of parallel molecular/electrophysiological analysis of cortical projection neurons (Nelson et al. 2006; Okaty et al. 2011b).

In the case of corticospinal neurons, it is possible that high I_h expression is involved in cortical mechanisms of motor control. We found that key functional properties of corticospinal neurons, which are likely to be physiologically relevant, were strongly I_h dependent. For one, corticospinal neurons resonated at ~4 Hz, compared with the lack of resonance observed in the other cell types. Intriguingly, a prominent peak at ~4 Hz has been observed in power spectra of local field potential recordings from multiple locations in the motor system in macaques, including primary motor cortex (Williams et al. 2010). If I_h contributes fundamentally to the integrative properties of corticospinal neurons, as our results imply, then I_h in corticospinal neurons is poised to influence how cortical circuits convey information to spinal circuits. Enhancing the appeal of this idea is the fact that I_h is under strong neuromodulatory regulation (Biel et al. 2009). Ascending noradrenergic, serotonergic, and dopaminergic projections are attractive candidates for up- and/or downregulating I_h in motor cortex pyramidal neurons (Barth et al. 2008; Carr et al. 2007; Foehring et al. 1989; Poolos et al. 2002). Neuromodulatory regulation of I_h could potentially be differentiated within or across projection classes and enable bidirectional control (Dembrow et al. 2010; Foehring et al. 1989; Spain 1994). We found that I_h in corticospinal neurons was decreased by α1- and α2-adrenergic agonists. Interestingly, the same agonists had no effect on the properties of corticostriatal or corticocortical neurons, suggesting that I_h is necessary for adrenergic sensitivity in cortical pyramidal neurons. However, adrenergic receptor expression levels, not explored here, could at least partially explain the difference in response to adrenergic agonists.

Abnormalities in neocortical I_h expression are associated with neurological disorders, such as epilepsy (Bender et al. 2003; Brewster et al. 2002; Chen et al. 2001; Dyhrfjeld-Johnsen et al. 2009; Huang et al. 2009; Jung et al. 2007; Kole et al. 2007; Marcelin et al. 2009; Santoro et al. 2010; Shah et al. 2004; Shin et al. 2008) and pain (Chaplan et al. 2003; Jiang et al. 2008; Luo et al. 2007). Our findings raise the possibility that alterations in I_h expression, function, or neuromodulatory control could be involved in diseases affecting corticospinal neurons too. Corticospinal neuron dysfunction occurs either primarily or secondarily in a wide variety of neurological disorders. The availability of experimental models for many of these—ranging from common ones, such as cerebrovascular disease and Parkinson's disease, to rarer but more corticospinal-specific ones, such as amyotrophic lateral sclerosis and hereditary spastic paraplegia (James and Talbot 2006; Tovar-Y-Romo et al. 2009)—will make it feasible to evaluate changes in corticospinal I_h as an etiological factor in these conditions.

Corticospinal-specific I_h as a Potential Microcircuit-Level Mechanism for Regulating Cortical Output to Spinal Cord

In the second part of this study, we developed and tested the idea that differential expression of I_h in motor cortex pyramidal neurons—in particular, high I_h expression in corticospinal neurons and low I_h expression in corticostriatal neurons—functions as a molecular-, cellular-, and microcircuit-level mechanism (or substrate), which enables the differential transfer of local circuit activity to divergent downstream channels in the motor system (e.g., corticospinal system vs. corticostriatal system). To test this idea, we used experimental paradigms involving stimulation of pyramidal neurons in the motor cortex while recording from retrogradely labeled corticospinal and corticostriatal neurons. These experiments allowed us to dissect various aspects of synaptic integration and to test the role of I_h in this process. We found that spatial and temporal synaptic integration of EPSPs from layer 2/3 pyramidal neurons was highly I_h dependent in corticospinal neurons and not in corticostriatal neurons. Thus our findings support a model in which I_h modulation selectively regulates the gain of the EPSP-to-AP transfer function in corticospinal neurons without affecting integration or activity in corticostriatal neurons.

This stands in contrast to alternative models (Fig. 12). For example, in a "balanced" model (Fig. 12*A*), activity would increase or decrease in both channels together, or in a "switching" model (Fig. 12*B*), the output of the motor cortex would be

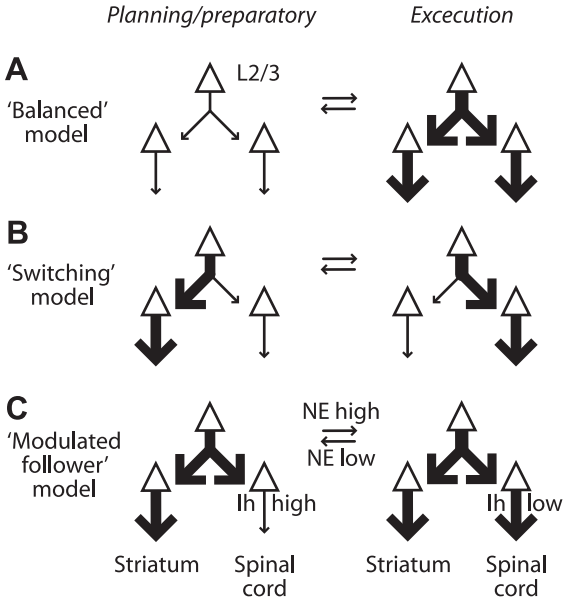

Fig. 12. Models for regulating the transfer of local circuit activity into corticospinal output during action planning vs. action execution. *A*: in a "Balanced" model, layer 2/3 synaptic input is equally distributed to corticospinal and corticostriatal pathways. *B*: in a "Switching" model, layer 2/3 synaptic input is differentially routed to the downstream channels. *C*: in a "Modulated follower" model, corticospinal-specific I_h selectively regulates translation of layer 2/3 inputs into outputs to spinal cord under neuromodulatory control by norepinephrine (NE).

differentially routed to divergent downstream channels in the motor system (e.g., output increasing to corticospinal but decreasing to corticostriatal and vice versa). Instead, our results suggest a "modulated follower" model (Fig. 12*C*), in which corticospinal neurons "listen" to local circuit activity with gain, which is variable due to I_h. Consistent with this, from circuit-mapping studies, it appears that corticospinal neurons project little if any synaptic output back into the local circuit in the motor cortex (Anderson et al. 2010; Weiler et al. 2008). Hodologically, they function more as intracortically situated "receivers" (or "antennae") for the spinal motor system. Their sensitivity to input and thus their output are modulated (by I_h), but their own activity may have little impact on the activity of other neurons in the motor cortex. An obvious caveat with our interpretation is that these experiments were performed in vitro, and therefore, it remains untested whether these findings pertain in vivo. We also note that in addition to the I_h-based model proposed here, other microcircuit-level mechanisms (representing various conceptual models) undoubtedly contribute to differentially regulating the output of motor cortex circuits to downstream motor systems.

That I_h can function as a variable attenuator of synaptic inputs to neocortical pyramidal neurons is well established from previous studies in other cortical areas and species [e.g., (Biel et al. 2009; Magee 1998)], including layer 5 pyramidal neurons in the rat somatosensory cortex (Berger et al. 2001; Berger and Lüscher 2003; Stuart and Spruston 1998). Blockade of I_h in brain slices of ferret PFC causes an increase in overall activity, presumably due to enhanced synaptic integration (Wang et al. 2007). Our studies differ in that we recorded from identified corticospinal and corticostriatal neurons in mouse motor cortex and specifically stimulated excitatory inputs from layer 2/3 pyramidal neurons (in contrast to current injection or nonspecific activation of axons of passage by electrical stimulation of cortical neuropil). Thus what is new in the present work is that we examined specific intracortical microcircuits (layer 2/3 → corticospinal), and we place our findings in the context of the motor system and specific hypotheses for intracortical mechanisms for motor control.

Although we specifically studied layer 2/3 inputs [the major source of local circuit excitatory input (Anderson et al. 2010)], we expect the results to generalize to other sources of both local and long-range input. Indeed, because I_h exerts bidirectional effects, counteracting both positive and negative excursions in membrane potential, the phenomena could apply to inhibitory inputs too (Chen et al. 2001). Our findings predict that inputs arriving at the apical dendritic arbors should show relatively large I_h-dependent effects, as detected at the soma (Fig. 4*E*, bottom plot, region *a*). Areas for further investigation include: *1*) experimental evaluation of the contributions of thalamic and neuromodulatory inputs and *2*) in vivo paradigms to evaluate the role of corticospinal I_h in modulating actual muscle activity in intact preparations.

Spatially, in contrast to the large relative effects of I_h in the apical tufts, the largest absolute differences were in the perisomatic region, consisting of basal and proximal apical dendritic branches. Indeed, several observations suggest a rather proximal site of action of I_h for the experimental paradigms used here. For example, the dampening effect of I_h occurred both for somatically injected αEPSPs (Fig. 7) and for EPSPs arriving in the dendritic arbor from layer 2/3 neurons (Fig. 8). Also, trains of inputs were similarly filtered by I_h, whether they arrived on the same (Fig. 8) or (presumably) different dendritic branches (Fig. 9). Higher resolution methods will be needed to understand the spatial dynamics of I_h in corticospinal neurons in detail. However, our data suggest that I_h, in proximal and basal dendrites, contributes substantially to dendritic integration in these neurons.

Temporally, the largest I_h-dependent differences in corticospinal neuron responses were for ISIs in the range of 25-75 ms, corresponding to frequencies of 13-40 Hz (β/γ range). In primate motor cortex, coherent oscillations in this range are implicated in regulating corticospinal activity during various aspects of motor behavior (Baker et al. 1999; Murthy and Fetz 1992; Schoffelen et al. 2005). Moreover, among different types of motor cortical neurons recorded in awake-behaving primates, those that demonstrate a characteristic rebound afterhyperpolarization (AHP) have been shown to have a tendency to fire at 25–35 Hz; this AHP may involve I_h (Chen and Fetz 2005). How corticospinal-specific I_h contributes to the regulation of the synaptic inputs, which underlie cortical oscillations during motor behavior, remains to be explored.

Ascending noradrenergic, serotonergic, and dopaminergic projections are candidates for up- and/or downregulating I_h in motor cortex pyramidal neurons. Neuromodulatory regulation of I_h could potentially be differentiated within or across projection classes (Foehring et al. 1989; Spain 1994). We have shown that I_h, in corticospinal neurons, is decreased by α-adrenergic agonists. Thus in terms of the proposed model, we speculate that activity in neuromodulatory inputs to the motor cortex would reduce I_h specifically in corticospinal neurons, thereby amplifying the impact of EPSPs and increasing the spiking output of these neurons to spinal cord circuits. This model shares core elements with a related model proposed for

regulating connectivity among pyramidal neurons in PFC through I_h modulation (Wang et al. 2007). In that model, stimulation of α2-adrenergic receptors closes HCN channels (decreasing I_h) and increases the efficacy of synaptic inputs, which strengthens the functional connectivity of PFC microcircuits. Autonomic activation in humans occurs during mental motor simulations, coincident with motor activity (Decety et al. 1993; Oishi et al. 1994). Our results suggest that I_h, as a downstream target of noradrenergic stimulation, is poised to adjust the functional connectivity of corticospinal microcircuits in motor cortex, thereby regulating the translation of action planning in intracerebral circuits into spinally directed motor commands.

We note that our findings and the model of I_h-dependent modulation of corticospinal output are compatible with systems-level models of motor control, such as models describing hierarchical and parallel processing across motor and frontal areas involved in action planning and execution [e.g., (Cohen et al. 2010; Smith et al. 2010)]. Indeed, an intriguing possibility is that this model applies more generally, i.e., that the I_h-dependent link from layer 2/3 to subcortical motor systems via brainstem/spinal cord-projecting neurons in layer 5B pertains across cortex.

ACKNOWLEDGMENTS

We thank C. Anderson and A. Apicella for assisting with surgeries, N. Yamawaki and D. Chen for comments and suggestions, and J. Yu for help with early experiments.

P. L. Sheets performed all experiments and analysis, with contributions from B. A. Suter, T. Kiritani, and G. M. G. Shepherd. C. S. Chan and D. J. Surmeier supervised quantitative PCR experiments and analysis. P. L. Sheets and G. M. G. Shepherd wrote the paper.

GRANTS

Support for this study was provided by National Institute of Neurological Disorders and Stroke (NS066675 to P. L. Sheets, NS069777 to C. S. Chan, NS047085 to D. J. Surmeier, and NS061963 and AG020506 to G. M. G. Shepherd), Whitehall Foundation (to G. M. G. Shepherd), and Parkinson's Disease Foundation and American Parkinson Disease Association Research (to C. S. Chan). Support for this work was also provided by the Northwestern University Robert H. Lurie Comprehensive Cancer Center Flow Cytometry Facility and a Cancer Center Support Grant (NCI CA060553).

DISCLOSURES

No conflicts of interest, financial or otherwise, are declared by the author(s).

REFERENCES

Anderson CT, Sheets PL, Kiritani T, Shepherd GM. Sublayer-specific microcircuits of corticospinal and corticostriatal neurons in motor cortex. *Nat Neurosci* 13: 739–744, 2010.

Baker SN, Kilner JM, Pinches EM, Lemon RN. The role of synchrony and oscillations in the motor output. *Exp Brain Res* 128: 109–117, 1999.

Barth AM, Vizi ES, Zelles T, Lendvai B. alpha2-Adrenergic receptors modify dendritic spike generation via HCN channels in the prefrontal cortex. *J Neurophysiol* 99: 394–401, 2008.

Beloozerova IN, Sirota MG, Swadlow HA. Activity of different classes of neurons of the motor cortex during locomotion. *J Neurosci* 23: 1087–1097, 2003a.

Beloozerova IN, Sirota MG, Swadlow HA, Orlovsky GN, Popova LB, Deliagina TG. Activity of different classes of neurons of the motor cortex during postural corrections. *J Neurosci* 23: 7844–7853, 2003b.

Bender RA, Soleymani SV, Brewster AL, Nguyen ST, Beck H, Mathern GW, Baram TZ. Enhanced expression of a specific hyperpolarization-activated cyclic nucleotide-gated cation channel (HCN) in surviving dentate gyrus granule cells of human and experimental epileptic hippocampus. *J Neurosci* 23: 6826–6836, 2003.

Berger T, Larkum ME, Lüscher HR. High I(h) channel density in the distal apical dendrite of layer V pyramidal cells increases bidirectional attenuation of EPSPs. *J Neurophysiol* 85: 855–868, 2001.

Berger T, Lüscher HR. Timing and precision of spike initiation in layer V pyramidal cells of the rat somatosensory cortex. *Cereb Cortex* 13: 274–281, 2003.

Betz V. Anatomischer Nachweis zweier Gehimcentra. *Centrlblatt für die medizinischen Wissenschaften* 12: 578–595, 1874.

Biel M, Wahl-Schott C, Michalakis S, Zong X. Hyperpolarization-activated cation channels: from genes to function. *Physiol Rev* 89: 847–885, 2009.

Bookout AL, Cummins CL, Mangelsdorf DJ, Pesola JM, Kramer MF. High-throughput real-time quantitative reverse transcription PCR. *Curr Protoc Mol Biol* Chapter 15: Unit 15.18, 2006.

Boucsein C, Nawrot M, Rotter S, Aertsen A, Heck D. Controlling synaptic input patterns in vitro by dynamic photo stimulation. *J Neurophysiol* 94: 2948–2958, 2005.

Brewster A, Bender RA, Chen Y, Dube C, Eghbal-Ahmadi M, Baram TZ. Developmental febrile seizures modulate hippocampal gene expression of hyperpolarization-activated channels in an isoform- and cell-specific manner. *J Neurosci* 22: 4591–4599, 2002.

Brown SP, Hestrin S. Cell-type identity: a key to unlocking the function of neocortical circuits. *Curr Opin Neurobiol* 19: 415–421, 2009a.

Brown SP, Hestrin S. Intracortical circuits of pyramidal neurons reflect their long-range axonal targets. *Nature* 457: 1133–1136, 2009b.

Carr DB, Andrews GD, Glen WB, Lavin A. alpha2-Noradrenergic receptors activation enhances excitability and synaptic integration in rat prefrontal cortex pyramidal neurons via inhibition of HCN currents. *J Physiol* 584: 437–450, 2007.

Catsman-Berrevoets CE, Lemon RN, Verburgh CA, Bentivoglio M, Kuypers HG. Absence of callosal collaterals derived from rat corticospinal neurons. A study using fluorescent retrograde tracing and electrophysiological techniques. *Exp Brain Res* 39: 433–440, 1980.

Chan CS, Glajch KE, Gertler TS, Guzman JN, Mercer JN, Lewis AS, Goldberg AB, Tkatch T, Shigemoto R, Fleming SM, Chetkovich DM, Osten P, Kita H, Surmeier DJ. HCN channelopathy in external globus pallidus neurons in models of Parkinson's disease. *Nat Neurosci* 14: 85–92, 2011.

Chaplan SR, Guo HQ, Lee DH, Luo L, Liu C, Kuei C, Velumian AA, Butler MP, Brown SM, Dubin AE. Neuronal hyperpolarization-activated pacemaker channels drive neuropathic pain. *J Neurosci* 23: 1169–1178, 2003.

Chen D, Fetz EE. Characteristic membrane potential trajectories in primate sensorimotor cortex neurons recorded in vivo. *J Neurophysiol* 94: 2713–2725, 2005.

Chen K, Aradi I, Thon N, Eghbal-Ahmadi M, Baram TZ, Soltesz I. Persistently modified h-channels after complex febrile seizures convert the seizure-induced enhancement of inhibition to hyperexcitability. *Nat Med* 7: 331–337, 2001.

Chen W, Zhang JJ, Hu GY, Wu CP. Electrophysiological and morphological properties of pyramidal and nonpyramidal neurons in the cat motor cortex in vitro. *Neuroscience* 73: 39–55, 1996.

Christophe E, Doerflinger N, Lavery DJ, Molnár Z, Charpak S, Audinat E. Two populations of layer V pyramidal cells of the mouse neocortex: development and sensitivity to anesthetics. *J Neurophysiol* 94: 3357–3367, 2005.

Churchland MM, Cunningham JP, Kaufman MT, Ryu SI, Shenoy KV. Cortical preparatory activity: representation of movement or first cog in a dynamical machine? *Neuron* 68: 387–400, 2010.

Cohen O, Sherman E, Zinger N, Perlmutter S, Prut Y. Getting ready to move: transmitted information in the corticospinal pathway during preparation for movement. *Curr Opin Neurobiol* 20: 696–703, 2010.

Day M, Carr DB, Ulrich S, Ilijic E, Tkatch T, Surmeier DJ. Dendritic excitability of mouse frontal cortex pyramidal neurons is shaped by the interaction among HCN, Kir2, and Kleak channels. *J Neurosci* 25: 8776–8787, 2005.

Decety J, Jeannerod M, Durozard D, Baverel G. Central activation of autonomic effectors during mental simulation of motor actions in man. *J Physiol* 461: 549–563, 1993.

Dembrow NC, Chitwood RA, Johnston D. Projection-specific neuromodulation of medial prefrontal cortex neurons. *J Neurosci* 30: 16922–16937, 2010.

Dyhrfjeld-Johnsen J, Morgan RJ, Soltesz I. Double trouble? Potential for hyperexcitability following both channelopathic up- and downregulation of I(h) in epilepsy. *Front Neurosci* 3: 25–33, 2009.

Foehring RC, Schwindt PC, Crill WE. Norepinephrine selectively reduces slow Ca2+- and Na+-mediated K+ currents in cat neocortical neurons. *J Neurophysiol* 61: 245–256, 1989.

Gao WJ, Zheng ZH. Target-specific differences in somatodendritic morphology of layer V pyramidal neurons in rat motor cortex. *J Comp Neurol* 476: 174–185, 2004.

Georgopoulos AP, Stefanis CN. The motor cortical circuit. In: *Handbook of Brain Microcircuits*, edited by Shepherd GM and Grillner S. New York: Oxford University Press, 2010, p. 39–45.

Hari R. Brain rhythms and reactivity of the human motor cortex. In: *Inter-Areal Coupling of Human Brain Function*. Excerpta Medica, International Congress Series 1226: 87–95 2002.

Harris NC, Constanti A. Mechanism of block by ZD 7288 of the hyperpolarization-activated inward rectifying current in guinea pig substantia nigra neurons in vitro. *J Neurophysiol* 74: 2366–2378, 1995.

Hattox AM, Nelson SB. Layer V neurons in mouse cortex projecting to different targets have distinct physiological properties. *J Neurophysiol* 98: 3330–3340, 2007.

Hooks BM, Hires SA, Zhang YX, Huber D, Petreanu L, Svoboda K, Shepherd GM. Laminar analysis of excitatory local circuits in vibrissal motor and sensory cortical areas. *PLoS Biol* 9: e1000572, 2011.

Huang Z, Walker MC, Shah MM. Loss of dendritic HCN1 subunits enhances cortical excitability and epileptogenesis. *J Neurosci* 29: 10979–10988, 2009.

Hutcheon B, Yarom Y. Resonance, oscillation and the intrinsic frequency preferences of neurons. *Trends Neurosci* 23: 216–222, 2000.

Isomura Y, Harukuni R, Takekawa T, Aizawa H, Fukai T. Microcircuitry coordination of cortical motor information in self-initiation of voluntary movements. *Nat Neurosci* 12: 1586–1593, 2009.

James PA, Talbot K. The molecular genetics of non-ALS motor neuron diseases. *Biochim Biophys Acta* 1762: 986–1000, 2006.

Jiang YQ, Xing GG, Wang SL, Tu HY, Chi YN, Li J, Liu FY, Han JS, Wan Y. Axonal accumulation of hyperpolarization-activated cyclic nucleotide-gated cation channels contributes to mechanical allodynia after peripheral nerve injury in rat. *Pain* 137: 495–506, 2008.

Jung S, Jones TD, Lugo JN Jr, Sheerin AH, Miller JW, D'Ambrosio R, Anderson AE, Poolos NP. Progressive dendritic HCN channelopathy during epileptogenesis in the rat pilocarpine model of epilepsy. *J Neurosci* 27: 13012–13021, 2007.

Kasper EM, Larkman AU, Lübke J, Blakemore C. Pyramidal neurons in layer 5 of the rat visual cortex. I. Correlation among cell morphology, intrinsic electrophysiological properties, and axon targets. *J Comp Neurol* 339: 459–474, 1994.

Kaufman MT, Churchland MM, Santhanam G, Yu BM, Afshar A, Ryu SI, Shenoy KV. Roles of monkey premotor neuron classes in movement preparation and execution. *J Neurophysiol* 104: 799–810, 2010.

Keller A. Intrinsic synaptic organization of the motor cortex. *Cereb Cortex* 3: 430–441, 1993.

Kole MH, Brauer AU, Stuart GJ. Inherited cortical HCN1 channel loss amplifies dendritic calcium electrogenesis and burst firing in a rat absence epilepsy model. *J Physiol* 578: 507–525, 2007.

Kole MH, Hallermann S, Stuart GJ. Single Ih channels in pyramidal neuron dendrites: properties, distribution, and impact on action potential output. *J Neurosci* 26: 1677–1687, 2006.

Larkum ME, Waters J, Sakmann B, Helmchen F. Dendritic spikes in apical dendrites of neocortical layer 2/3 pyramidal neurons. *J Neurosci* 27: 8999–9008, 2007.

Le Bé JV, Silberberg G, Wang Y, Markram H. Morphological, electrophysiological, and synaptic properties of corticocallosal pyramidal cells in the neonatal rat neocortex. *Cereb Cortex* 17: 2204–2213, 2007.

Lei W, Jiao Y, Del Mar N, Reiner A. Evidence for differential cortical input to direct pathway versus indirect pathway striatal projection neurons in rats. *J Neurosci* 24: 8289–8299, 2004.

Lemon RN. Descending pathways in motor control. *Annu Rev Neurosci* 31: 195–218, 2008.

Lewis AS, Schwartz E, Chan CS, Noam Y, Shin M, Wadman WJ, Surmeier DJ, Baram TZ, Macdonald RL, Chetkovich DM. Alternatively spliced isoforms of TRIP8b differentially control h channel trafficking and function. *J Neurosci* 29: 6250–6265, 2009.

Lewis AS, Vaidya SP, Blaiss CA, Liu Z, Stoub TR, Brager DH, Chen X, Bender RA, Estep CM, Popov AB, Kang CE, Van Veldhoven PP, Bayliss DA, Nicholson DA, Powell CM, Johnston D, Chetkovich DM. Deletion of the hyperpolarization-activated cyclic nucleotide-gated channel auxiliary subunit TRIP8b impairs hippocampal Ih localization and function and promotes antidepressant behavior in mice. *J Neurosci* 31: 7424–7440, 2011.

Llinás R. The intrinsic electrophysiological properties of mammalian neurons: insights into nervous system function. *Science* 242: 1654–1664, 1988.

Lorincz A, Notomi T, Tamas G, Shigemoto R, Nusser Z. Polarized and compartment-dependent distribution of HCN1 in pyramidal cell dendrites. *Nat Neurosci* 5: 1185–1193, 2002.

Losonczy A, Zemelman BV, Vaziri A, Magee JC. Network mechanisms of theta related neuronal activity in hippocampal CA1 pyramidal neurons. *Nat Neurosci* 13: 967–972, 2010.

Luo L, Chang L, Brown SM, Ao H, Lee DH, Higuera ES, Dubin AE, Chaplan SR. Role of peripheral hyperpolarization-activated cyclic nucleotide-modulated channel pacemaker channels in acute and chronic pain models in the rat. *Neuroscience* 144: 1477–1485, 2007.

Lüthi A, McCormick DA. H-current: properties of a neuronal and network pacemaker. *Neuron* 21: 9–12, 1998.

Magee JC. Dendritic hyperpolarization-activated currents modify the integrative properties of hippocampal CA1 pyramidal neurons. *J Neurosci* 18: 7613–7624, 1998.

Magee JC. Dendritic Ih normalizes temporal summation in hippocampal CA1 neurons. *Nat Neurosci* 2: 508–514, 1999.

Marcelin B, Chauviere L, Becker A, Migliore M, Esclapez M, Bernard C. h Channel-dependent deficit of theta oscillation resonance and phase shift in temporal lobe epilepsy. *Neurobiol Dis* 33: 436–447, 2009.

Mason A, Larkman A. Correlations between morphology and electrophysiology of pyramidal neurons in slices of rat visual cortex. II. Electrophysiology. *J Neurosci* 10: 1415–1428, 1990.

Miller MN, Okaty BW, Nelson SB. Region-specific spike-frequency acceleration in layer 5 pyramidal neurons mediated by Kv1 subunits. *J Neurosci* 28: 13716–13726, 2008.

Molnár Z, Cheung AF. Towards the classification of subpopulations of layer V pyramidal projection neurons. *Neurosci Res* 55: 105–115, 2006.

Moosmang S, Biel M, Hofmann F, Ludwig A. Differential distribution of four hyperpolarization-activated cation channels in mouse brain. *Biol Chem* 380: 975–980, 1999.

Morishima M, Kawaguchi Y. Recurrent connection patterns of corticostriatal pyramidal cells in frontal cortex. *J Neurosci* 26: 4394–4405, 2006.

Murthy VN, Fetz EE. Coherent 25- to 35-Hz oscillations in the sensorimotor cortex of awake behaving monkeys. *Proc Natl Acad Sci USA* 89: 5670–5674, 1992.

Narayanan R, Johnston D. Long-term potentiation in rat hippocampal neurons is accompanied by spatially widespread changes in intrinsic oscillatory dynamics and excitability. *Neuron* 56: 1061–1075, 2007.

Nelson SB, Hempel C, Sugino K. Probing the transcriptome of neuronal cell types. *Curr Opin Neurobiol* 16: 571–576, 2006.

Nicoll A, Larkman A, Blakemore C. Modulation of EPSP size and efficacy by intrinsic membrane conductances in rat neocortical pyramidal neurons in vitro. *J Physiol* 468: 693–710, 1993.

Notomi T, Shigemoto R. Immunohistochemical localization of Ih channel subunits, HCN1–4, in the rat brain. *J Comp Neurol* 471: 241–276, 2004.

Oishi K, Kimura M, Yasukawa M, Yoneda T, Maeshima T. Amplitude reduction of H-reflex during mental movement simulation in elite athletes. *Behav Brain Res* 62: 55–61, 1994.

Okaty BW, Sugino K, Nelson SB. A quantitative comparison of cell-type-specific microarray gene expression profiling methods in the mouse brain. *PLoS One* 6: e16493, 2011a.

Okaty BW, Sugino K, Nelson SB. Cell type-specific transcriptomics in the brain. *J Neurosci* 31: 6939–6943, 2011b.

Özdinler PH, Macklis JD. IGF-I specifically enhances axon outgrowth of corticospinal motor neurons. *Nat Neurosci* 9: 1371–1381, 2006.

Petreanu L, Huber D, Sobczyk A, Svoboda K. Channelrhodopsin-2-assisted circuit mapping of long-range callosal projections. *Nat Neurosci* 10: 663–668, 2007.

Phillips CG, Porter R. *Corticospinal Neurones: Their Role in Movement*. London: Academic Press, 1977.

Poolos NP, Migliore M, Johnston D. Pharmacological upregulation of h-channels reduces the excitability of pyramidal neuron dendrites. *Nat Neurosci* 5: 767–774, 2002.

Press C, Cook J, Blakemore SJ, Kilner J. Dynamic modulation of human motor activity when observing actions. *J Neurosci* 31: 2792–2800, 2011.

Reiner A. Organization of corticostriatal projection neuron types. In: *Handbook of Basal Ganglia Structure and Function: A Decade of Progress*, edited by Steiner H and Tseng KY, 2010.

Reiner A, Hart NM, Lei W, Deng Y. Corticostriatal projection neurons—dichotomous types and dichotomous functions. *Front Neuroanat* 4: 142, 2010.

Robinson RB, Siegelbaum SA. Hyperpolarization-activated cation currents: from molecules to physiological function. *Annu Rev Physiol* 65: 453–480, 2003.

Roth M, Decety J, Raybaudi M, Massarelli R, Delon-Martin C, Segebarth C, Morand S, Gemignani A, Decorps M, Jeannerod M. Possible involvement of primary motor cortex in mentally simulated movement: a functional magnetic resonance imaging study. *Neuroreport* 7: 1280–1284, 1996.

Santoro B, Lee JY, Englot DJ, Gildersleeve S, Piskorowski RA, Siegelbaum SA, Winawer MR, Blumenfeld H. Increased seizure severity and seizure-related death in mice lacking HCN1 channels. *Epilepsia* 51: 1624–1627, 2010.

Santoro B, Piskorowski RA, Pian P, Hu L, Liu H, Siegelbaum SA. TRIP8b splice variants form a family of auxiliary subunits that regulate gating and trafficking of HCN channels in the brain. *Neuron* 62: 802–813, 2009.

Santoro B, Wainger BJ, Siegelbaum SA. Regulation of HCN channel surface expression by a novel C-terminal protein-protein interaction. *J Neurosci* 24: 10750–10762, 2004.

Schmittgen TD, Livak KJ. Analyzing real-time PCR data by the comparative C(T) method. *Nat Protoc* 3: 1101–1108, 2008.

Schoffelen JM, Oostenveld R, Fries P. Neuronal coherence as a mechanism of effective corticospinal interaction. *Science* 308: 111–113, 2005.

Schubert D, Staiger JF, Cho N, Kötter R, Zilles K, Luhmann HJ. Layer-specific intracolumnar and transcolumnar functional connectivity of layer V pyramidal cells in rat barrel cortex. *J Neurosci* 21: 3580–3592, 2001.

Shah MM, Anderson AE, Leung V, Lin X, Johnston D. Seizure-induced plasticity of h channels in entorhinal cortical layer III pyramidal neurons. *Neuron* 44: 495–508, 2004.

Sheets PL, Shepherd GM. Cortical circuits for motor control. *Neuropsychopharmacology* 36: 365–366, 2011.

Shepherd GM. Intracortical cartography in an agranular area. *Front Neurosci* 3: 337–343, 2009.

Shepherd GMG. Circuit mapping by ultraviolet uncaging of glutamate. In: *Imaging in Neuroscience: A Laboratory Manual*, edited by Helmchen F, Konnerth A, and Yuste R. Cold Spring Harbor, NY: Cold Spring Harbor Laboratory, 2011, p. 417–427.

Shepherd GMG, Pologruto TA, Svoboda K. Circuit analysis of experience-dependent plasticity in the developing rat barrel cortex. *Neuron* 38: .277–289, 2003.

Shin M, Brager D, Jaramillo TC, Johnston D, Chetkovich DM. Mislocalization of h channel subunits underlies h channelopathy in temporal lobe epilepsy. *Neurobiol Dis* 32: 26–36, 2008.

Smith NJ, Horst NK, Liu B, Caetano MS, Laubach M. Reversible inactivation of rat premotor cortex impairs temporal preparation, but not inhibitory control, during simple reaction-time performance. *Front Integr Neurosci* 4: 124, 2010.

Spain WJ. Serotonin has different effects on two classes of Betz cells from the cat. *J Neurophysiol* 72: 1925–1937, 1994.

Spain WJ, Schwindt PC, Crill WE. Anomalous rectification in neurons from cat sensorimotor cortex in vitro. *J Neurophysiol* 57: 1555–1576, 1987.

Stafstrom CE, Schwindt PC, Crill WE. Negative slope conductance due to a persistent subthreshold sodium current in cat neocortical neurons in vitro. *Brain Res* 236: 221–226, 1982.

Stafstrom CE, Schwindt PC, Flatman JA, Crill WE. Properties of subthreshold response and action potential recorded in layer V neurons from cat sensorimotor cortex in vitro. *J Neurophysiol* 52: 244–263, 1984.

Stamos AV, Savaki HE, Raos V. The spinal substrate of the suppression of action during action observation. *J Neurosci* 30: 11605–11611, 2010.

Stuart G, Spruston N. Determinants of voltage attenuation in neocortical pyramidal neuron dendrites. *J Neurosci* 18: .3501–3510, 1998.

Sugino K, Hempel CM, Miller MN, Hattox AM, Shapiro P, Wu C, Huang ZJ, Nelson SB. Molecular taxonomy of major neuronal classes in the adult mouse forebrain. *Nat Neurosci* 9: 99–107, 2006.

Suter BA, O'Connor T, Iyer V, Petreanu LT, Hooks BM, Kiritani T, Svoboda K, Shepherd GMG. Ephus: multipurpose data acquisition software for neuroscience experiments. *Front Neural Circuits* 4: 1–12, 2010.

Tovar-Y-Romo LB, Santa-Cruz LD, Tapia R. Experimental models for the study of neurodegeneration in amyotrophic lateral sclerosis. *Mol Neurodegener* 4: 31, 2009.

Tseng GF, Prince DA. Heterogeneity of rat corticospinal neurons. *J Comp Neurol* 335: 92–108, 1993.

Turner RS, DeLong MR. Corticostriatal activity in primary motor cortex of the macaque. *J Neurosci* 20: 7096–7108, 2000.

van Aerde KI, Mann EO, Canto CB, Heistek TS, Linkenkaer-Hansen K, Mulder AB, van der Roest M, Paulsen O, Brussaard AB, Mansvelder HD. Flexible spike timing of layer 5 neurons during dynamic beta oscillation shifts in rat prefrontal cortex. *J Physiol* 587: 5177–5196, 2009.

Wahl-Schott C, Biel M. HCN channels: structure, cellular regulation and physiological function. *Cell Mol Life Sci* 66: 470–494, 2009.

Wang M, Ramos BP, Paspalas CD, Shu Y, Simen A, Duque A, Vijayraghavan S, Brennan A, Dudley A, Nou E, Mazer JA, McCormick DA, Arnsten AF. alpha2A-Adrenoceptors strengthen working memory networks by inhibiting cAMP-HCN channel signaling in prefrontal cortex. *Cell* 129: 397–410, 2007.

Watakabe A. Comparative molecular neuroanatomy of mammalian neocortex: what can gene expression tell us about areas and layers? *Dev Growth Differ* 51: 343–354, 2009.

Weiler N, Wood L, Yu J, Solla SA, Shepherd GMG. Top-down laminar organization of the excitatory network in motor cortex. *Nat Neurosci* 11: 360–366, 2008.

Williams ER, Soteropoulos DS, Baker SN. Spinal interneuron circuits reduce ~10-Hz movement discontinuities by phase cancellation. *Proc Natl Acad Sci USA* 107: 11098–11103, 2010.

Williams SR, Mitchell SJ. Direct measurement of somatic voltage clamp errors in central neurons. *Nat Neurosci* 11: 790–798, 2008.

Williams SR, Stuart GJ. Site independence of EPSP time course is mediated by dendritic I(h) in neocortical pyramidal neurons. *J Neurophysiol* 83: 3177–3182, 2000.

Wood L, Gray NW, Zhou Z, Greenberg ME, Shepherd GM. Synaptic circuit abnormalities of motor-frontal layer 2/3 pyramidal neurons in an RNA interference model of methyl-CpG-binding protein 2 deficiency. *J Neurosci* 29: 12440–12448, 2009.

Yu J, Anderson CT, Kiritani T, Sheets PL, Wokosin DL, Wood L, Shepherd GM. Local-circuit phenotypes of layer 5 neurons in motor-frontal cortex of YFP-H mice. *Front Neural Circuits* 2: 1–8, 2008.